Thompson-Like Groups for Dendrite Julia Sets

A Senior Project submitted to
The Division of Science, Mathematics, and Computing
of
Bard College

by
Will Smith

Annandale-on-Hudson, New York
May, 2013

Abstract

We develop a Thompson-like group for the Julia set associated to the polynomial $z^2 + i$, in a similar manner as the Thompson group for the Basilica developed by Belk and Forrest. This Julia set is a dendrite, and we include a discussion of the geometric branching structure that arises as a result. We prove that this group is finitely generated and give explicit generators for it. Also, we show that the commutator subgroup has infinite index by way of showing that the group has an infinite cyclic quotient. Additionally, we find that this group contains isomorphic copies of the modular group, Thompson's group F, and two diagram groups of interest . Finally, we develop a scheme for generalizing this group to act on other dendrite Julia sets, and conjecture that, in those cases, the groups found will have properties similar to this one.

Contents

List of Figures

Dedication

For all of you still catching your breath. JG, DM, SF, LB, HR, JWB, CE, HJ, GM, JP, SL, and LM.

Acknowledgments

Many thanks to Jim Belk, my advisor, without whom this project would have been a shambles. Jim's enthusiasm and clarity throughout the work on this project ensured that, at its conclusion, it is approaching the best project it could be.

I also owe a great deal to Lauren Rose, without whom I would not be a math major.

Also, for their support and kindness to me this whole year, I want to thank Eleanor Reid, Mary Caponegro, Beth Hoffman-Patalona, Nick O'Leary, Ari Brown, my parents, the rest of my family, and everybody named in the dedication.

Finally, many thanks to anybody that ever pretended to be interested when I talked about this project, not to mention anybody that actually was. You know who you are.

Introduction

The present research is a generalization of research presented by Belk and Forrest in [1]; their work is in turn a generalization of Thompson's groups F, T, and V. Thompson's groups F, T, and V are groups of piecewise-linear homeomorphisms of the unit interval, the unit circle, and the Cantor set, respectively, which arise from dyadic subdivisions of those sets. Because the process of repeatedly halving those sets is dependent on their self-similarity, it seemed logical to attempt to define a similar sort of group acting on a Julia set; Belk and Forrest did so, defining a group called T_B, which acts on the Basilica (the Julia set for $z^2 - 1$). They were able to prove a number of results about it, including that it is finitely generated and that the commutator subgroup is simple. They have also defined similar groups acting two other Julia sets, known as the Douady rabbit and the airplane, and proved similar results for those.

In this project, we investigate another such group called T_D that acts on the Julia set for the map $\phi(z) = z^2 + i$, which is a dendrite, meaning that it has a tree-like branching structure, and no interior. Proving analogous results for the dendrite turned out to be surprisingly difficult. In comparison to T_B, which has large copies of T inside of it, no

particularly useful copies of any other groups could be found inside of T_D, which meant that much of our work needed to be developed from scratch. Additionally, because the dendrite has no interior, all but countably many points of the dendrite are pinch points, which makes a number of things much more complicated than in the case of the Basilica or the rabbit. In particular, it is much more difficult to define a notion of two pinch points being adjacent, since the pinch points are dense on the dendrite, so between any two lie infinitely many more. Additionally, where the lamination for the Basilica has large gaps in it that occur where the interior regions lie, the dendrite lamination has no such gaps, and in fact has a stucture similar to that of a Cantor set. This again complicates the investigation, and makes the lamination a much more difficult object to deal with.

In spite of this, we were able to successfully develop a number of results to our satisfaction. The first major result we proved was that T_D is finitely generated. The proof of this is much more complicated than the corresponding proof for the Basilica group, because, as mentioned, where T_B, has large copies of T inside of it, no useful copies of any other groups could be found inside of T_D, which meant our proof needed to be entirely original. The final version of the proof uses an inductive argument on the number of objects in the reduced arc pair diagram for a function, wherein we show that our generators can be used to simplify any function down to nothing; hence, working backwards, the function can be constructed using nothing but the generators. The second major result we found was a proof that the abelianization of T_D is infinite, and is in fact virtually cyclic. For the Basilica group, a two-coloring of the interior regions of the Julia set provided a homomorphism to $\mathbb{Z}/2$, but in T_D, because there are no interior regions, such a map was not available. Our argument that the abelianization of T_D is infinite depends instead on an examination of the slopes around certain points of the piecewise-linear functions that generate T_D. To show that it is virtually cyclic, we found an onto homomorphism to $\mathbb{Z}$, and showed that it is a quotient of $\mathbb{Z} \times \mathbb{Z}/2 \times \mathbb{Z}/3$.

In addition to these results, we also found copies of the modular group, Thompson's group F, and two interesting diagram groups inside of T_D. The map to the modular group is dependent on the fact that the dendrite has a branching structure that contains an infinite tree that is a copy of the one that Γ acts on. The map to F is predicated on the fact that, because it has no interior, the dendrite behaves in some ways more like a line segment than a circle, and we use this structure to find corresponding dyadic subdivisions.

The final work of the project was the idea that this group might be generalized to other dendrites. Because many dendrites share a similar structure to that of the $c = i$ dendrite, it seems quite plausible that a group very like T_D might act on them. In the final chapter, we present a scheme for generalizing T_D to groups that act on other dendrites, which we call T_D^*, and conjecture that the results we found for T_D will also hold for T_D^*, in some analogous form.

In Chapter 1, we present preliminaries about Julia sets, Thompson's groups F, T and V, and give an overview of Belk and Forrest's group for the Basilica. In Chapter 2, we introduce the dendrite and go to some lengths to develop an understanding of its structure, as well as develop the tools necessary to define T_D. In Chapter 3, we present T_D, and develop our main results, and in Chapter 4, we present our conjectures about T_D^*.

1
Preliminaries

1.1 Julia Sets and the Mandelbrot Set

We will give here an overview of Julia sets. A Julia set is obtained through repeated iteration of a function in $\mathbb{C}$; hence, we need a definition of the **orbit** of a point under such iteration.

Definition 1.1.1. Let A be a set, let $x \in A$, and let $f : A \to A$ be a function. Then the **orbit** of x under f is the set of points $\{f(x), f(f(x)), \dots\}$ that are obtainable as $f^n(x)$ for some $n \in \mathbb{N}$.

We can then use this to give a definition of a filled Julia set. We will give the definition of the Julia set proper shortly; it follows from this definition.

Definition 1.1.2. Let $c \in \mathbb{C}$. Then the **filled Julia set** for c, denoted J, is the set of all points whose orbit under the polynomial $z^2 + c$ remains bounded.

To better understand Julia sets, we will consider two examples.

Example 1.1.3. Consider the filled Julia set for $c = 0$. This is the set of all points whose orbit under the polynomial $f(z) = z^2$ remains bounded. It is simple to see that this is the

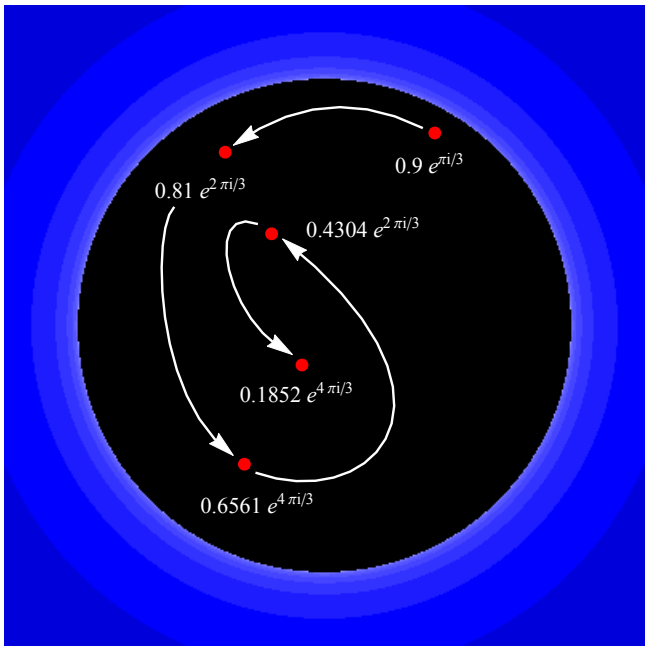

Figure 1.1.1: A subset of the orbit of $.9e^{\pi i/3}$

closed unit disc: for any $z \in \mathbb{C}$ so that $|z| \leq 1$, we see that $|z^2| \leq |z|$, and for all $z \in \mathbb{C}$ so that $|z| > 1$, $|z^2| > |z|$. Thus, points that lie on or within the unit circle will remain there under any number of iterations of z^2, and points with absolute value greater than 1 will be mapped to points with even larger absolute values, and eventually diverge to infinity.

Observe in Figure 1.1.1 that the orbit of $.9e^{\pi i/3}$ remains bounded under the map z^2.

We now present the definition of a Julia set.

Definition 1.1.4. Let $c \in \mathbb{C}$. Then the **Julia set** for c, denoted ∂J, is the topological boundary of the filled Julia set for c.

Observe that the points that lie on the unit circle are always mapped to other points on the unit circle. It turns out that in every filled Julia set this is the case; the Julia set for any polynomial p is invariant under p.

Now we will consider another example.

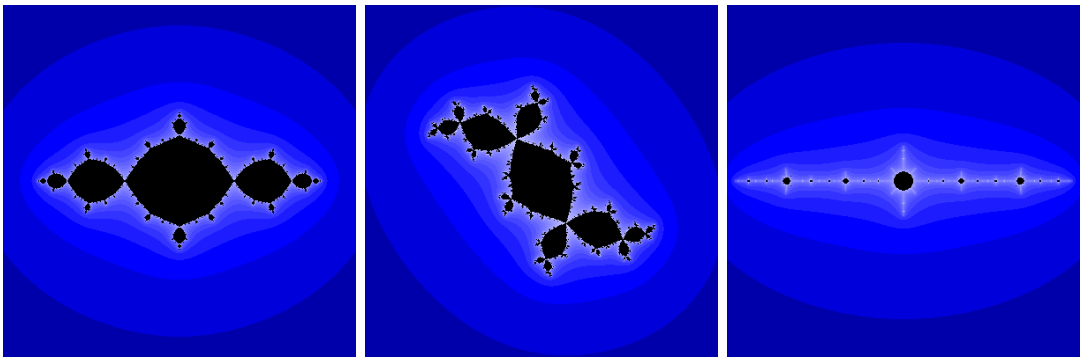

Figure 1.1.2: The Basilica (left), the Douady rabbit (center), and the airplane (right).

Example 1.1.5. Let B be the Julia set for $c = -1$, corresponding to the polynomial $z^2 - 1$, shown in Figure 1.1.2. The Julia set B is known as the Basilica, so named for its resemblance to the St. Mark's Basilica in Venice. Note that, in spite of its much more complicated shape, the points that lie on the boundary of the filled Basilica; that is, the Julia set itself, are always mapped to other boundary points under the mapping $z^2 - 1$.

Example 1.1.6. Another significant Julia set is the one for $c = -1/8 + 3/4i$, shown in Figure 1.1.2, which is known as the Douady Rabbit. Aside from being a canonical example of a Julia set, the rabbit is of particular interest here because its structure is in many ways analogous to that of the Julia set that is the subject of the present research.

Example 1.1.7. A final example that merits consideration is the Julia set for $c = -1.755$, shown in Figure 1.1.2, which we refer to as the airplane. The airplane is of interest because it has been the subject of more analogous research to this present work, by Belk and Forrest.

It is also important to note that, while the Basilica and the Rabbit have pinch points between their interior regions, the interior regions are all connected. Thus, we say that they, as well as the Airplane, are is path-connected, which we define here.

Definition 1.1.8. Let U be a set, and let $p, q \in U$. Then a **path** from p to q is a continuous function $\gamma : [0,1] \longrightarrow U$ such that $\gamma(0) = p$ and $\gamma(1) = q$.

Definition 1.1.9. Let U be a set. Then U is **path-connected** if for each distinct $x, y \in U$, there exists a path from x to y in U.

We also give a definition of total disconnectedness, which is intuitively the opposite of path-connectedness.

Definition 1.1.10. Let U be a set. Then U is **totally disconnected** if for each distinct $x, y \in U$, there is not a path from x to y that lies within U.

These definitions lead to an important result about Julia sets, which is due to Mandelbrot.

Theorem 1.1.11. *(Dichotomy Theorem) Let $c \in \mathbb{C}$. Then the Julia set for c is either connected or totally disconnected, and it is connected if and only if the orbit of zero under the map $z^2 + c$ remains bounded.*

This theorem is presented in Section 4 of [2], and is proved therein.

Example 1.1.12. Consider the Julia set for $c = 1$, shown in Figure 1.1.3. This Julia set is comprised of what seem to be clusters of dust in the complex plane; we will use the above criterion to verify that it is, indeed, totally disconnected. Consider the orbit of zero:

$$f(0) = 1$$

$$f(f(0)) = f(1) = 2$$

$$f(f(f(0))) = f(2) = 5$$

$$f^{(4)}(0) = f(5) = 26$$

$$\vdots$$

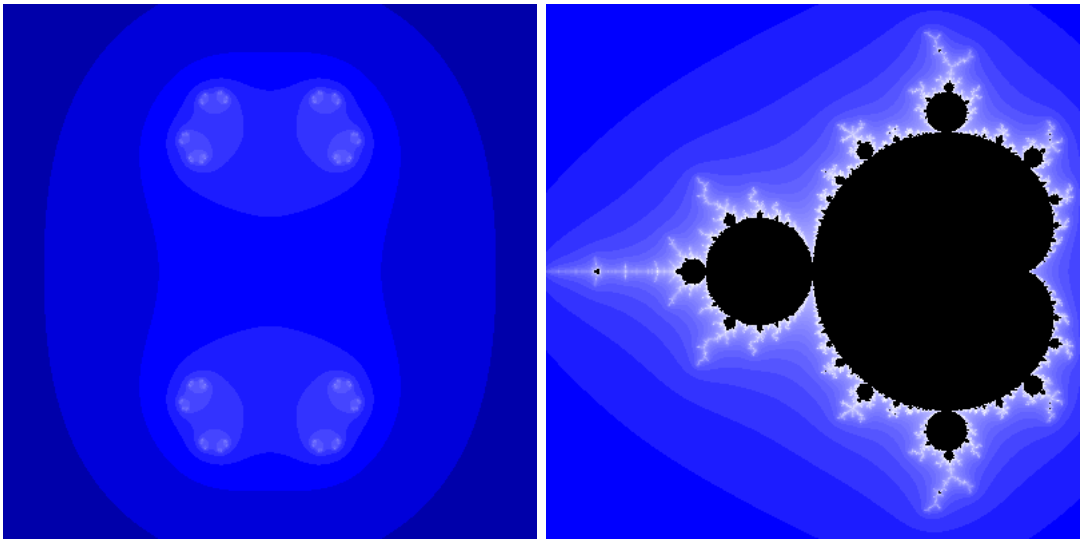

Figure 1.1.3: Left: The Julia set for $z^2 + 1$ is totally disconnected. Right: The Mandelbrot Set

This orbit produces a sequence of natural numbers that is clearly diverging. Since any real number greater than 1, when squared, becomes larger, and since c is positive, it is clear that the sequence is monotone increasing, so it must go to infinity. Thus, the Julia set for $c = 1$ is totally disconnected.

The notion of dichotomy for Julia sets leads us to the last definition for this section, which begins to produce a way of organizing some of the complexity generated by Julia sets.

Definition 1.1.13. The **Mandelbrot set**, shown in Figure 1.1.3 is the set of all points $c \in \mathbb{C}$ such that the Julia set for $z^2 + c$ is connected.

While Julia sets are very repetitive in their structure–they have the fractal property of being the same on many scales–the Mandelbrot set is much more complex, and difficult to make sense of. Nonetheless, giving an image of it helps us begin to develop some insight about its nature.

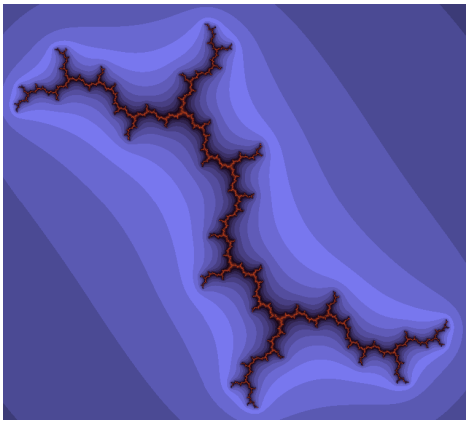

Figure 1.2.1: The dendrite.

1.2 Dendrites

My research is primarily concerned with a class of Julia sets called **dendrites**. Intuitively, dendrites are a family of Julia sets that have no interior, and display a tree-like branching structure. Formally, dendrites have a definition that is topological, and not dependent on their being Julia sets.

Definition 1.2.1. A **dendrite** is a topological space X with the following properties:

- X is compact
- X is connected
- X is locally connected
- X contains no simple closed curves

Now we have another definition.

Definition 1.2.2. A **dendrite Julia set** is a Julia set that is also a dendrite.

Example 1.2.3. Consider the Julia set for $c = i$, shown in Figure 1.2.1. Morosawa, Nishimura, Taniguchi, and Ueda verify in Example 1.1.5 of [6] that this is a dendrite, and

we will not go through the proof here. Observe, however, that it displays the branching structure that is typical of dendrites, and that, from a sense of visual intuition, there should be no simple closed curves, assuming that on smaller scales, the structure continues to be the same as it does on larger scales, which it does. Note that this is the Julia set that is the primary focus of this project, and in general, the phrase "the dendrite" will refer to it, unless otherwise specified.

With a view to the second question, of how to find dendrites, we now introduce some definitions and a theorem.

Definition 1.2.4. Let $f : \mathbb{C} \to \mathbb{C}$ be a polynomial. Then f is **post-critically finite** if the orbits of all critical points of f are finite.

In particular, for polynomials of the form $z^2 + c$, the only critical point is 0, so we need only verify that the orbit of zero is finite for such a polynomial to be post-critically finite. We now introduce a related definition, that of periodicity of points under a mapping.

Definition 1.2.5. Let $f : \mathbb{C} \to \mathbb{C}$ be a polynomial, and let $p \in \mathbb{C}$. Then p is **periodic** with respect to f if there is some $n \in \mathbb{N}$ so that $f^n(p) = p$.

Example 1.2.6. To illustrate these two definitions, we observe that the polynomial $z^2 - 1$, which corresponds to the Basilica, is post-critically finite, since the orbit of zero under that mapping is the stable two-cycle $\{0, -1\}$.

We are now able to state a definition that will be important in studying dendrite Julia sets.

Definition 1.2.7. Let $c \in \mathbb{C}$. Then c is a **Misiurewicz point** if $z^2 + c$ is post-critically finite, and zero is pre-periodic with respect to that mapping; that is, zero is not periodic, but there is a least one point in the orbit of zero that is periodic.

It turns out that the Julia sets that correspond to Misiurewicz points are always dendrites [6]. We can use this fact to generate some more examples of dendrites by solving various polynomial equations to produce values of c that are Misiurewicz points.

To illustrate this, we give the following proposition.

Proposition 1.2.8. *Let $c \in \mathbb{C}$. Then if 0 is not periodic under the map $f(z) = z^2 + c$, and $f^2(0)$ has period two, then $c = \pm i$.*

Proof. The way we find a point that satisfies these conditions is by letting $c \in \mathbb{C}$, and $f : \mathbb{C} \to \mathbb{C}$ the polynomial $f(z) = z^2 + c$, and solving for c when we set the condition

$$f(f(0)) = f(f(f(f(0)))).$$

This is equivalent to saying that we have

$$((0)^2 + c)^2 + c = ((((0)^2 + c)^2 + c)^2 + c)^2 + c$$

so

$$c^2 + c = ((c^2 + c)^2 + c)^2 + c.$$

It turns out this equation has roots at $0, -1, -2, i$ and $-i$. However, when $c = 0$, $f(0) = 0$, so zero itself is periodic, and thus, 0 is not a Misiurewicz point. Similarly, when $c = -1$, $f(0) = -1$, and $f(-1) = 0$, so again, zero is periodic, and -1 is not a Misiurewicz point. We can see, though, that for $c = -2$, the orbit of zero is $0 \to -2 \to 2 \to 2 \to \ldots$. Thus, zero is preperiodic, and -2 is indeed a Misiurewicz point. Note that the fact that it satisfies our above requirement is actually incidental, since the second iterate of 0 actually has period one, rather than period two.

Now consider the case when $c = i$, We see that the orbit of zero is then $0 \to i \to -1 + i \to -i \to -1 + i \to \ldots$, so indeed the second iterate of zero is periodic, with period two. Similarly, in the case where $c = -i$, we see that the orbit of zero is $0 \to -i \to -1 - i \to -i$

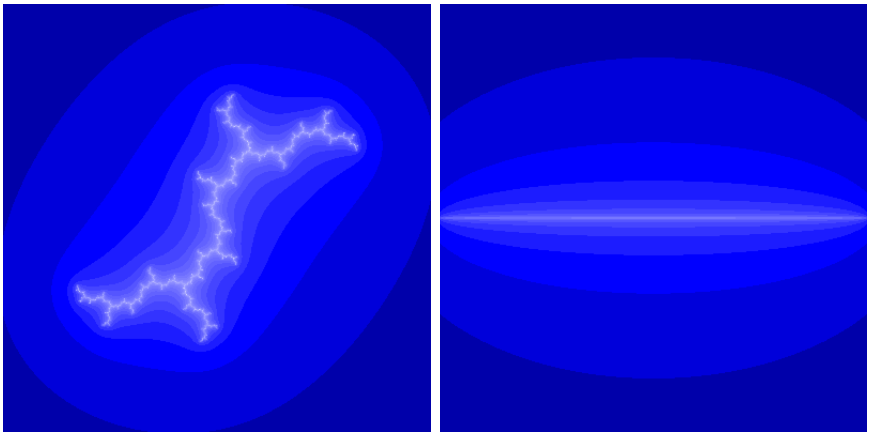

Figure 1.2.2: Left: The dendrite for $c = -i$. Right: The Julia set for $c = -2$.

$\to -1 - i \to \ldots$, so again the second iterate of zero is periodic, with period two. Thus, both i and $-i$ are Misiurewicz points, with the requirement above satisfied as desired. □

We now consider the Julia sets given by the three Misiurewicz points we have obtained. We have already seen the Julia set for $c = i$; it is the dendrite seen in Figure 1.2.1. It turns out that the Julia set for $c = -i$ is just the reflection of that dendrite across the real axis, as we see in Figure 1.2.2 left. The Julia set for $c = -2$ is somewhat strange in that it is indeed a dendrite, but by virtue of the fact that it consists entirely of the interval $[-2, 2]$ in the real line, seen in Figure 1.2.2 right. More dendrites can be obtained in a similar manner, by simply choosing other requirements on which point in the orbit of zero should be periodic, and what the period of it should be, and solving for c in the same way. Because this is how Misiurewicz points are constructed, this will always yield a dendrite.

1.3 Thompson's Groups F, T and V

In [3], Richard Thompson introduced three infinite groups, called F, T, and V. Many attempts have been made to generalize these groups, of which the present research is one. In this section I present a brief overview of Thompson's groups, and then in the next,

explain their relation to [1] of Belk and Forrest. Because the function of Thompson's groups here is only one of motivation, rather than structure, the discussion of them will serve only as a brief overview; a more in-depth discussion of them can be found in [4].

We begin with an explanation of **dyadic subdivisions**. Start with the unit interval:

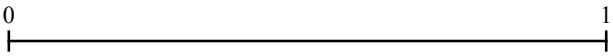

Divide it in two at the midpoint:

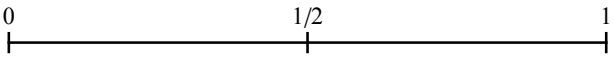

Then the two pieces are both homeomorphic to the original interval. Divide each of these in two at their midpoints, and divide some more of the resulting intervals at their respective midpoints, stopping after a finite number of steps:

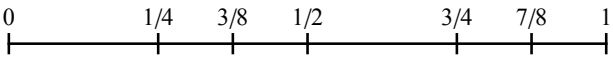

The resulting partition is a **dyadic subdivision** of the unit interval.

Definition 1.3.1. A **dyadic subdivision** of the unit interval is a partition of the unit interval that is created by cutting it into halves a finite number of times.

Thompson's group *F* is a group of piecewise-linear functions mapping the unit interval to itself. These functions are formed by choosing two dyadic subdivisions of the unit interval that have the same number of breakpoints and mapping one to the other piecewise-linearly. It turns out that this group is both finitely generated and finitely presented, and that its commutator subgroup is simple.

Elements of F can be described in the standard way of writing piecewise functions; that is, we can write an element of F as

$$X_0(x) = \begin{cases} 1/2x & \text{if } 0 \leq x \leq 1/2 \\ x - 1/4 & \text{if } 1/2 \leq x \leq 3/4 \\ 2x - 1/4 & \text{if } 3/4 \leq x \leq 1. \end{cases}$$

However, this is often not the most productive way to describe such functions. Cannon, Floyd and Parry, in [4] employ "rectangle diagrams" to give a visual intuition about elements of F. For example, the function X_0 given above corresponds in a fairly obvious way to the following diagram:

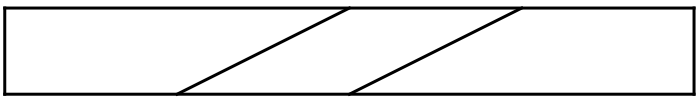

In this way, with the top side of the rectangle representing the domain of the function, and the bottom representing the range, we are provided with a fairly good intuition about such functions. As another example, consider the following rectangle diagram for a function called X_1:

We could no doubt produce a piecewise definition of this function, but to do so would not benefit us enormously here, so we will not.

Proposition 1.3.2. *The functions X_0 and X_1 generate Thompson's group F.*

The proof of this proposition can be found in [4].

Thompson's group T is a group of piecewise-linear functions mapping the unit circle to itself, with the same restrictions as before. That is, we label points on the unit circle with numbers in $[0, 1]$, and then define dyadic subdivisions in the same way as before. Then elements of T are defined in the same way as elements of F. The important difference between F and T is that because T acts on the unit circle, elements may rotate around the circle, in addition to simply scaling and sliding along the interval. Examples of such functions can be found in Figure 1.3.1.

In the same way that functions in F can be written in the standard form for piecewise functions, we can write elements of T as piecewise functions with output in $\mathbb{R} \mod 1$.

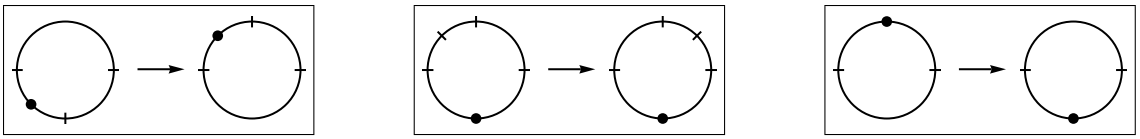

Figure 1.3.1: Generators for T. Note that in each, a point is marked in both the domain and range pictures to specify the map. Originally from [1].

But, as before, we are often better served by a diagram that gives a visual intuition about such functions. In Figure 1.3.1 we have three such diagrams. Observe that, while in F, there was never ambiguity about which piece of the interval in the domain was mapped to which piece in the range, because elements of T may rotate around the circle, it is necessary to mark a point in the domain and range of each function to specify the map. It is clear that, if necessary, one could construct a piecewise definition of these functions, but we will not do that here. Also note that the third function serves as an example of an element of T that is only comprised of rotation. We present the following theorem summarizing important results about T:

Theorem 1.3.3. *1. T is finitely generated. In particular, T is generated by the three dyadic rearrangements shown in Figure 1.3.1.*

2. T is simple.

3. T is finitely presented.

The proof of these statements can be found in [4].

1.4 The Böttcher Map and Caratheodory Loop

In this section and the next, we develop some of the standard tools for marking location on Julia sets. It is ultimately our goal to define, in the manner of James Belk and Bradley Forrest in [1], a group of piecewise-linear homeomorphisms from the dendrite to itself. To do this, however, we need these tools. The first is a theorem that provides a correspondence

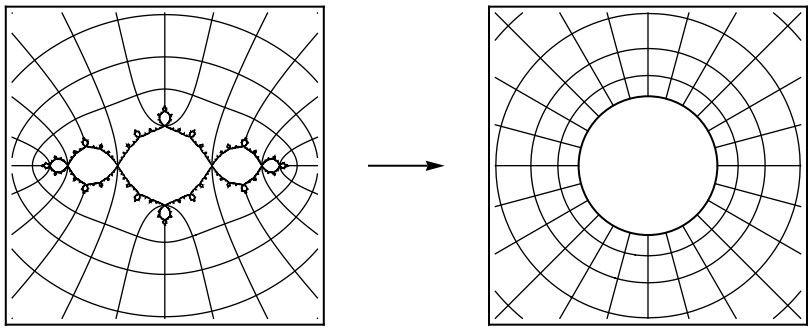

Figure 1.4.1: The Böttcher Map for the Basilica. Originally from [1]

between points in the complement of the filled Julia set for some quadratic polynomial, and points in the complement of the closed unit disk. We then use this to describe a surjective mapping from the unit circle to the Julia set proper, by which correspondence it is made much easier to mark location on the Julia set.

Theorem 1.4.1. *Let J be a filled Julia set for some quadratic polynomial f for which the Julia set J is connected. Then there exists an analytic bijection, known as the* ***Böttcher map*** *for J, $\Phi : \hat{\mathbb{C}} - J \longrightarrow \hat{\mathbb{C}} - D^2$ such that $\Phi(f(z)) = \Phi(z)^2$ for all $z \in \mathbb{C}$.*

Proof. We give only the sketch of a proof for this theorem. Consider a path-connected filled Julia set, J. In particular, we are interested in the complement of J in the Riemann sphere, which we denote $\hat{\mathbb{C}} - J$. By the Riemann mapping theorem, we know there must exist an analytic bijection from $\hat{\mathbb{C}} - J$ to the open unit disk, V. By convention, however, we prefer the mapping to the complement of the closed unit disk D^2, which we denote $\Phi : \hat{\mathbb{C}} - J \longrightarrow \hat{\mathbb{C}} - D^2$, which we can easily see exists by composing the inverse of the mapping $\hat{\mathbb{C}} - D^2 \longrightarrow V$ that the Riemann mapping theorem provides with our original mapping $\hat{\mathbb{C}} - J \longrightarrow V$. It is more difficult to prove the existence of a map with the requirement that $\Phi(f(z)) = \Phi(z)^2$; a more complete proof can be found in [2]. □

We want to use this mapping to give a correspondence between points on the unit circle and points on the Julia set. But since neither of those sets are involved in the

Böttcher map, we need to do a little bit more work to extend the mapping. Milnor gives the following theorems in [7]. Note that Theorems 1.4.3 and 1.4.4 make reference to the term 'subhyperbolic' as a property that a function may possess. Milnor gives the following definition of subhyperbolic.

Definition 1.4.2. The rational map f is **subhyperbolic** if it is expanding with respect to some orbifold metric on a neighborhood of its Julia set [7].

Because we only use the term as a stepping-stone from Theorem 1.4.3 to Theorem 1.4.4, we will cheerfully continue without concerning ourselves very much about what that means.

Theorem 1.4.3. *(Theorem* 19.6 *of* [7]*) A rational map is subhyperbolic if and only if every critical orbit is either finite or converges to an attracting periodic orbit.*

In particular, we can see that this means that any postcritically finite map is subhyperbolic; hence, the Basilica and the dendrite are given by subhyperbolic mappings.

Theorem 1.4.4. *(Theorem* 19.7 *of* [7]*) If f is subhyperbolic with ∂J connected, then ∂J is locally connected.*

Again, this can be applied to show that the Basilica and the dendrite are locally connected. This allows us to use the following theorem as desired.

Theorem 1.4.5. *(Theorem* 18.3 *of* [7]*) For any given f with connected Julia set, the following are equivalent.*

- *The Julia set ∂J is locally connected.*
- *The inverse Böttcher map $\Phi^{-1} : \hat{\mathbb{C}} - D^2 \longrightarrow \hat{\mathbb{C}} - J$ extends continuously over the boundary ∂D, and carries points in ∂D to points in ∂J.*

Now, when f is postcritically finite, we can then extend Φ by the inclusion mappings from each of $\hat{\mathbb{C}} - J$ and $\hat{\mathbb{C}} - D^2$ to their closures, and make the following diagram commute:

$$\begin{array}{ccc} \hat{\mathbb{C}} - J & \xleftarrow{\Phi^{-1}} & \hat{\mathbb{C}} - D^2 \\ \Big\downarrow \text{inclusion} & & \Big\downarrow \text{inclusion} \\ \overline{\hat{\mathbb{C}} - J} & \xleftarrow{\overline{\Phi}^{-1}} & \overline{\hat{\mathbb{C}} - D^2}. \end{array}$$

Because the closure of $\hat{\mathbb{C}} - J$ is equal to $(\hat{\mathbb{C}} - J) \cup \partial J$, and the closure of $\hat{\mathbb{C}} - D^2$ is equal to $(\hat{\mathbb{C}} - D^2) \cup S^1$, where S^1 is the unit circle, we can then restrict the map $\overline{\Phi}^{-1}$ to a mapping $\psi : S^1 \to \partial J$. This mapping is called the **Caratheodory loop**. It turns out that ψ is both continuous and surjective; in consequence of which, because both S^1 and ∂J are compact Hausdorff spaces, ψ is a quotient map, and ∂J is a quotient of S^1. Note that ψ will generally not be injective; as will be developed later, points in ∂J that have multiple preimages in S^1 are called **pinch points**, and exist in most Julia sets.

1.5 External Rays

The Böttcher map and Caratheodory loop are extremely useful for determining locations on the Julia sets. In particular, we describe objects called **external rays** as follows:

Definition 1.5.1. Let ∂J be a Julia set, and let Φ be the Böttcher map for ∂J. Then the images of radial lines, under the mapping from $\hat{\mathbb{C}} - D^2$ to $\hat{\mathbb{C}} - J$ are called **external rays** for ∂J.

By convention, we describe the angles of external rays using real numbers in $[0, 1]$. We can also consider the **landing points** of external rays.

Definition 1.5.2. Let ∂J be a Julia set, and let ψ be the caratheodory loop for ∂J. A point $t \in \partial J$ is the **landing point** for an external ray at angle θ if $\psi(\theta) = t$.

We also occasionally refer to the **external angles** of a point; this simply refers to the angles of the external rays that land on that point. Now we are able to give a formal definition of a pinch point in the terms we prefer to use.

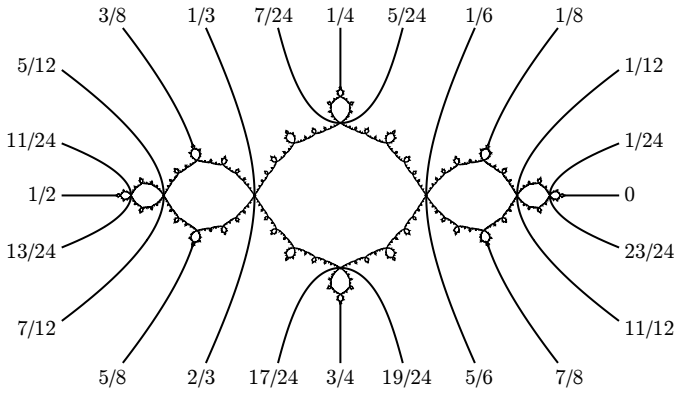

Figure 1.5.1: The External Rays for the Basilica. Originally from [1].

Definition 1.5.3. A **pinch point** on a Julia set is a point that is a landing point for more than one external ray.

It is quite common for us to denote a point by the angles of the external rays that land on it. Thus, as we will see, we would indicate the left main pinch point on the Basilica by the notation $\{1/3, 2/3\}$. We will illustrate these concepts by means of two examples.

Example 1.5.4. Consider the Basilica, the external rays of which are shown in Figure 1.5.1. We see that the pinch points for the Basilica are points that have external rays at angles that are rational numbers of the form

$$\frac{3k-1}{3\cdot 2^n} \quad \text{and} \quad \frac{3k+1}{3\cdot 2^n}$$

for some $k, n \in \mathbb{N}$.

In particular, the pinch point between the central interior region and the large region to the left of the central region has external rays at $1/3$ and $2/3$, and the pinch point between the central region and the large region to the right of the central region has external rays at $5/6$ and $1/6$. Also observe the intuitive reason that pinch points are so named; the removal of a pinch point will separate the Julia set into two or more pieces.

1.6 Laminations

As we have seen, the Caratheadory loop is a quotient map, by which a Julia set is a quotient of a circle. Because it is in general not injective, we can use that quotient to define an object called an **invariant lamination** which gives a visual representation of the equivalence relation of points in the circle that map to the same point on the Julia set.

Definition 1.6.1. A **hyberpolic arc** is a circular arc intersecting the unit circle that intersects the unit circle at right angles.

Between any two points on the circle (other than opposite points) there exists a hyperbolic arc.

Definition 1.6.2. An **invariant lamination** for a Julia set, ∂J is an object consisting of the closed unit disk, together with hyperbolic arcs that connect any two points whose image under ψ are equal.

More intuitively, we can say that the arcs of the invariant lamination connect any two points whose external rays land on the same point on the Julia set. A visual notion for the fact that the Basilica is a quotient of the circle by this lamination is the fact that if one were to contract every arc to a single point, the result would be the Basilica, with the arcs as pinch points, and the gaps as interior regions.

Example 1.6.3. Again consider the Basilica. We have already seen the structure of the external rays for the Basilica; we can use this information to construct the invariant lamination without too much difficulty. We begin with the unit circle, and then add arcs connecting 1/3 and 2/3, 1/6 and 5/6, and each other pair of rational numbers with the form $\frac{3k-1}{2\cdot 2^n}$ and $\frac{3k+1}{3\cdot 2^n}$, as described above. When we have finished, we have produced the invariant lamination for the Basilica, shown in Figure 1.6.1.

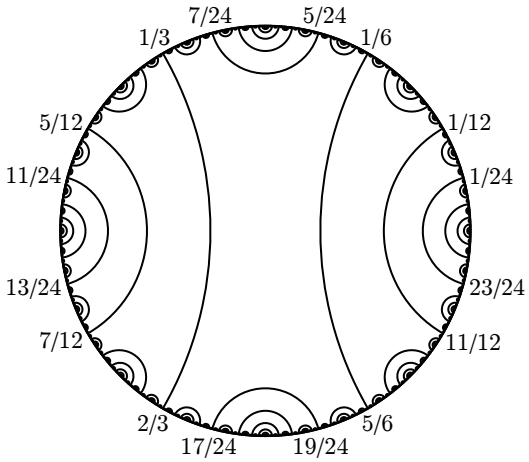

Figure 1.6.1: The Invariant Lamination for the Basilica. Originally from [1].

1.7 Finite Arc Diagrams, Arc Pair Diagrams, and Piecewise-Linear Homeomorphisms

Having constructed the invariant lamination for the Basilica, we observe that finite subsets of the lamination subdivide the unit circle in a manner somewhat analogous to the dyadic subdivisions of the circle seen in the elements of T. Thus, intuitively, we would like to describe maps that move one finite subset of the lamination to another isomorphic finite subset of the lamination, and thus, preserve the lamination overall. To do this, however, we must first more cautiously construct these finite subsets of the lamination.

We begin with the unit circle [1].

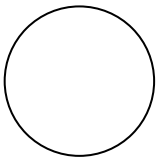

To this, we add the arcs $\{1/3, 2/3\}$ and $\{1/6, 5/6\}$ [1].

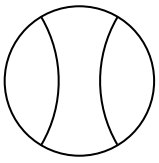

These arcs partition the circle into four segments, namely, $[-1/6, 1/6]$, $[1/6, 1/3]$, $[1/3, 2/3]$, and $[2/3, 5/6]$. In each of these segments, which we call **gaps**, we can place another arc, called the **primary arc** for that gap, which divides the gap in a ratio of $1 : 2 : 1$ [1].

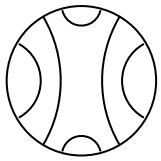

After continuing for some finite number of steps, choosing whether or not to insert the primary arc in each gap, we obtain a finite subset of the invariant lamination for the Basilica, which we call an **arc diagram**.

Now we wish to construct maps between such arc diagrams. To do this, we need a notion of what arc diagrams can be mapped to each other. In [1] Belk and Forrest give the following definition.

Definition 1.7.1. Let A and B be arc diagrams. Then A and B are **isomorphic** if, when viewed as 2-complexes, there exists an orientation-preserving isomorphism between the complexes.

Given such an isomorphism, then, there is a corresponding piecewise-linear homeomorphism of the circle that preserves the Basilica lamination. Such a homeomorphism is called a **dyadic rearrangement** of the Basilica, and the pair of arc diagrams, as illustrated in Figure 1.7.1 is called an **arc pair diagram**. Note that a corresponding pair of points have been marked in the domain and range pictures in order to specify the isomorphism. Arc pair diagrams are the standard tool for illustrating dyadic rearrangements of the Basilica, and will be used frequently.

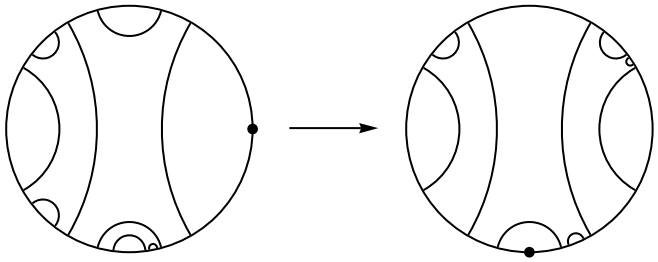

Figure 1.7.1: An isomorphic pair of arc diagrams. Originally from [1].

1.8 The Group T_B

The present exposition thus far has been in the service of allowing us to describe the main results of Belk and Forrest in [1], which we will summarize in this section. We denote the set of all dyadic rearrangements of the Basilica by T_B, and immediately present their first main result.

Theorem 1.8.1. *(Theorem 5.4 of* [1]*) Let f be a piecewise-linear homeomorphism of the circle. Then f induces a dyadic rearrangment of the Basilica if and only if it satisfies the following requirements:*

(1) *The Basilica lamination is invariant under f.*

(2) *Every breakpoint of f is the endpoint of an arc in the lamination.*

In particular, T_B forms a group under composition.

The next result begins to give some insight into the structure of the group T_B.

Theorem 1.8.2. *(Immediate from Theorem* 6.3 *of* [1]*) There is a subgroup of T_B isomorphic to Thompson's group T.*

Theorem 6.3 of [1] actually gives more information than this about the isomorphic subgroup in question. In simpler terms, it states that there is a copy of T that acts on the central component of the Basilica; that is, the interior region containing zero. Thus, the interior regions adjacent to the central component can be translated as by elements of T.

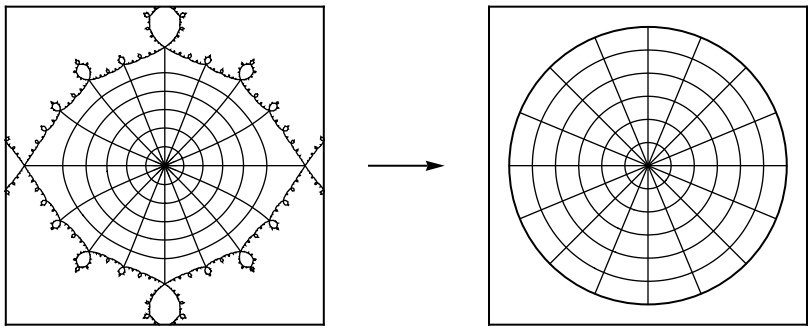

Figure 1.8.1: A Riemann map on the central component. Originally from [1].

Figure 1.8.1 provides an illustration of the correspondence between the central component and the unit circle. The Riemann map illustrated is used to form the image of T in T_B.

The fact that T_B contains this copy of T in so central a position simplifies the search for a generating set. In particular, Belk and Forrest proved that the elements that generate the copy of T contained in T_B, combined with one additional element of T_B form a generating set. Those elements are defined by the break points of their domain and range pictures as follows:

Name	Domain Breakpoints	Range Breakpoints
α	$1/3, 2/3$	$1/6, 5/6$
β	$1/6, 2/3, 17/24, 5/6$	$1/6, 7/24, 1/3, 5/6$
γ	$1/6, 7/24, 29/96, 1/3$	$1/6, 19/96, 5/24, 1/3$

They additionally define a fourth homeomorphism, called δ by the rule $\delta(\theta) = \theta + 1/2$. The actions of these four elements on the Basilica is illustrated in 1.8.2. Observe that β, γ and δ are the images of the generators for T mapped into the isomorphic subgroup in T_B. From these, Belk and Forrest have the following result.

Theorem 1.8.3. *(Theorem* 7.1 *of* [1]*) The group T_B is generated by the elements $\{\alpha, \beta, \gamma, \delta\}$.*

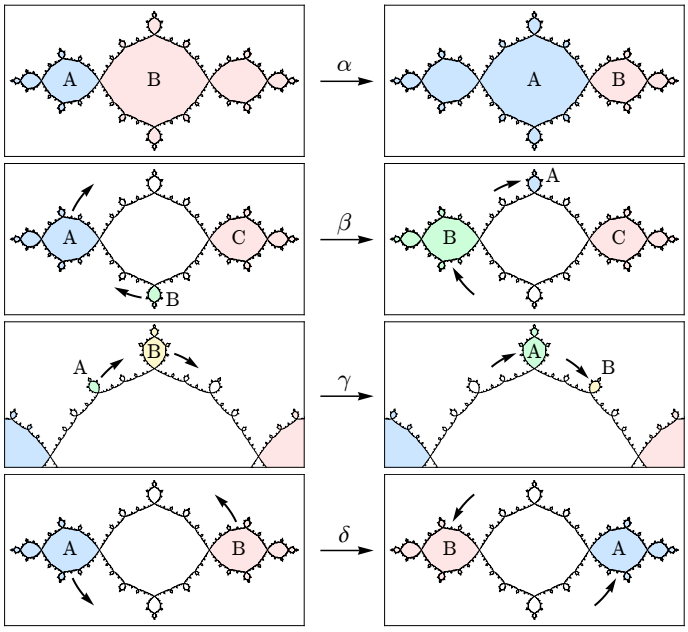

Figure 1.8.2: The actions of α, β, γ, and δ on the Basilica. Originally from [1].

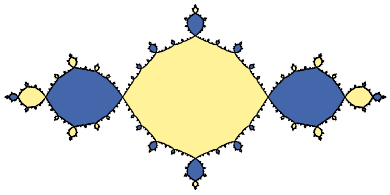

Figure 1.8.3: The two-coloring of the Basilica. Originally from [1].

We now present three more main results of [1] in a somewhat more abbreviated fashion. There exists a two-coloring of the Basilica, illustrated in Figure 1.8.3. Belk and Forrest used this to prove the following result about the commutator subgroup of T_B.

Theorem 1.8.4. *(Theorem 8.1 of* [1]*) The commutator subgroup* $[T_B, T_B]$ *is the index-two subgroup of* T_B *consisting of all elements that preserve the two-coloring of the Basilica.*

Additionally, Belk and Forrest proved the following two results about the structure of T_B.

Theorem 1.8.5. *(Corollary* 8.2 *of* [1]*) The abelianization of* T_B *is isomorphic to* $\mathbb{Z}/2\mathbb{Z}$.

Theorem 1.8.6. *(Theorem* 8.3 *of* [1]*) The group* $[T_B, T_B]$ *is simple.*

This last theorem is of particular interest, because being simple or having a simple commutator subgroup seems to be characteristic of Thompson's groups (recall T and V are simple, and the commutator subgroup, $[F, F]$ of F is simple), lending credence to the idea that T_B is a natural generalization of Thompson's groups.

In the next chapter, we begin with a further discussion of the dendrite for $c = i$, and begin to introduce the main work of the present research, a group called T_D that acts on that dendrite in a manner similar to that in which T_B acts on the Basilica.

2
The Dendrite

2.1 The Julia set for c = i

The majority of the effort in the present work has been directed towards a group that is similar to the Belk-Forrest group T_B, which acts on the dendrite corresponding to the map $\phi(z) = z^2 + i$, rather than on the Basilica. In order to develop the tools necessary to describe this group, we begin this chapter with an informal examination of the structure of this dendrite. All of the definitions in this section will be made formal in section 2.2.

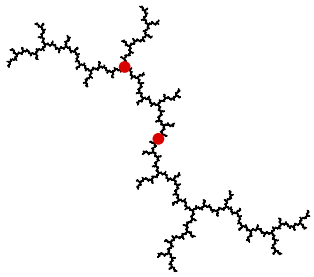

Figure 2.1.1: The Julia Set for $c = i$, known as the dendrite, with the central pool and main triple point marked.

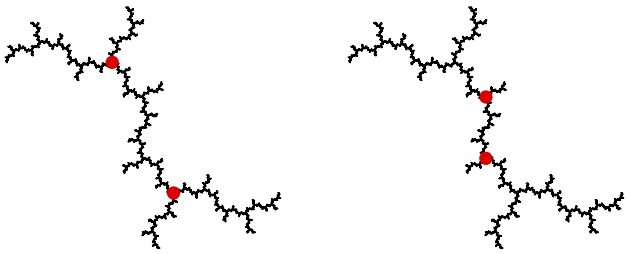

Figure 2.1.2: Two pairs of triple points on the dendrite converging to the central pool.

The first thing to observe about the dendrite is that it possesses, as noted earlier, a tree-like branching structure, and that, as well, it has no interior. These two facts alone set it very much in contrast to the Basilica and the Rabbit, neither of which can be said to have a tree-like structure, and both of which certainly have interiors. To better understand the branching of the dendrite, it can be helpful to choose one point to think of as the "center" of the dendrite, and examine the patterns that arise as one travels along a path on the dendrite away from that point. There are certainly a great many valid choices for such a point; in this section, we will look at two.

The first point to consider is the point located at $z = 0$, marked in Figure 2.1.1. This seems to be an obvious choice, since it is geometrically the center of the dendrite; a one-half rotation around this point maps the dendrite to itself. We refer to this point as the **central pool**. It will turn out to be the case that, even though this seems to be the most central point of the dendrite, there is another point that will be be a better choice of center. The reason, in particular, that this is not so good a choice of center, is that the dendrite does not branch at all at the central pool. Certainly it is a pinch point—because the dendrite has no interior, every point on the dendrite is a pinch point—but if you were traveling along a path on the dendrite, and came to the central pool, there would be no decision to make as to which way to go.

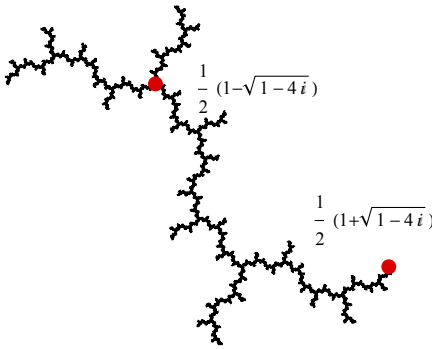

Figure 2.1.3: The Fixed Points of the Dendrite

In a sense, the central pool marks the space between branching points. To make sense of this claim, observe that the section of the dendrite located between the two branching points marked in the first image in Figure 2.1.2 looks a lot like the section of the dendrite located between the points marked in the second image. It turns out that inside the second section, there is another section with the same structure, and inside that, another. In fact, there is an infinite sequence of pairs of branching points that converge to the central pool—in each pair, one branches upward, and one branches downward—and the central pool is the point in the middle of all of them that doesn't branch at all. We will return to this structure, but now we will introduce the second candidate for the central point of the dendrite.

The next point we will consider is the point located at $z = \frac{1}{2}(1 - \sqrt{1-4i})$, which is also marked in Figure 2.1.1. Because this is a solution to the equation $z = z^2 + i$, this point is fixed under the $\phi = z^2 + i$ map. For this reason, it is known as the **fixed point** of the dendrite. There is actually a second point that is fixed under ϕ, located at $z = \frac{1}{2}(1+\sqrt{1-4i})$, but because, as we see in Figure 2.1.3, it lies on an end of the dendrite, it is of less interest to us. In general, when we speak of the fixed point, it will refer to the point at $\frac{1}{2}(1 - \sqrt{1-4i})$. More frequently, however, we will refer to it as the **main triple**

point, because it is a point at which the dendrite branches in three directions, and we have chosen it to be the most important such point. Its negation, $-z = -1 \cdot \frac{1}{2}(1-\sqrt{1-4i})$, is not fixed under the mapping, but the dendrite does also branch in three directions at this point. We say that any such point, where the dendrite branches in three directions, is a **triple point**, and in particular, we refer to the negation of the fixed point as the **lower triple point**.

There are two branching structures we will discuss that appear when traveling outward from the fixed point, but first we will mention one other term. An **arm** of a triple point is a subset of the dendrite that would be one of three connected components were that triple point removed (recall the definition of a pinch point). In particular, the **main arm** is the upward-pointing arm of the main triple point. The first structure we will discuss is that which lies between two triple points. In particular, consider the section of the dendrite that lies between the main triple point and the lower triple point. Along the path, or geodesic, between these points, there are many other triple points. In fact, the triple points are dense in the dendrite, and we will give a sketch of a proof of this later. In particular, though, observe that there are two triple points whose corresponding arms are larger than any others, and that the arm attached to the left one points upward, and the arm attached to the right one points downward. This is a pattern that repeats everywhere in the dendrite: between two triple points, there is an up arm and a down arm that are in some sense dominant on that region. Note that while in many cases it is obvious which two arms this should refer to, it is not always so well-defined. For example, in Figure 2.1.4, it is not at all clear which arms should be chosen. Nonetheless, it is often useful to be aware of this pattern.

Also note that in any case when this pattern does hold easily, there is again a sequence of pairs of triple points, like the sequence converging to the central pool described above, which converge to a point that lies directly between the two triple points. Any such point

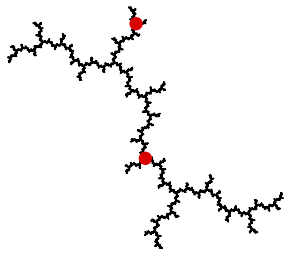

Figure 2.1.4: A pair of points without obvious arms between them.

we refer to as a **pool**, having as it does, in some sense, a similar structure to that of the central pool. Any section of the dendrite between two triple points on which the one-up, one-down pattern of arms is clearly defined, we will refer to as a **segment**, though we will define this term more precisely in the next section.

The second branching structure we will discuss is that of the entire arm in any direction. For example, consider the main arm of the fixed point. On any arm, there is a unique triple point that has larger arms attached to it than any other on that arm. This point for the main arm is marked in Figure 2.1.5. In general, we call this the **dominant triple point** for an arm. Note that, in general, between the triple point that is the base of an arm and the dominant triple point for that arm, the pattern of one arm up, one arm down that we just discussed will be readily apparent. Also note that the lower triple point is the dominant triple point for one arm of the main triple point, which arm comprises most of the dendrite. The characteristic pattern that we wish to discuss here is the fact that in most cases, the size of the arms of a triple point increase (mod the third arm) as one rotates counterclockwise around the triple point. That is, usually the second-smallest arm is located one-third of the way counterclockwise from the smallest arm, and the largest arm is again a third of the way counterclockwise from that. There are certainly points for which this does not hold, such as the point marked in Figure 2.1.5; nonetheless, it is worthwhile to be aware of this pattern. Also, one can find subsets of the set of triple points

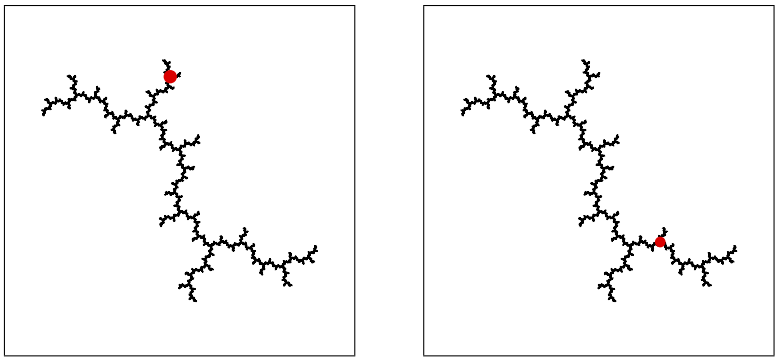

(a) (b)

Figure 2.1.5: (a) The Dominant Triple point for the main arm. (b) A point for which the seize of the arms increases clockwise.

for which it does always hold, such as the set generated by considering all the dominant triple points of arms attached to the main triple points, and then the dominant triple points of arms attached to those, and so on. There is a certain class of arm on which this pattern holds that we will refer to as a **branch arms**; these are the arms that have the same structure as the arms of the main triple point. As with segments, we will make this notion more precise in the next section.

In the cases of both of these patterns, there have been points for which the pattern seems to break down; this has very much to do with the fact that these patterns have not been at all rigorously stated, and we have made little attempt to avoid that so far. The goal of this section is primarily to develop some intuition about the structure of the dendrite, in order to enable a freer (though still rigorous) discussion of it later. Examining more where these patterns do and do not hold is often a good way into learning more about the real structure of the dendrite. For example, we will see later that the set of nested dominant points described above corresponds to a subgroup of the group studied in this project that will turn out to be isomorphic to the modular group Γ. The places where the patterns hold nicely will often be of interest to us, and the places where the patterns break down, we will find we must tread more carefully around.

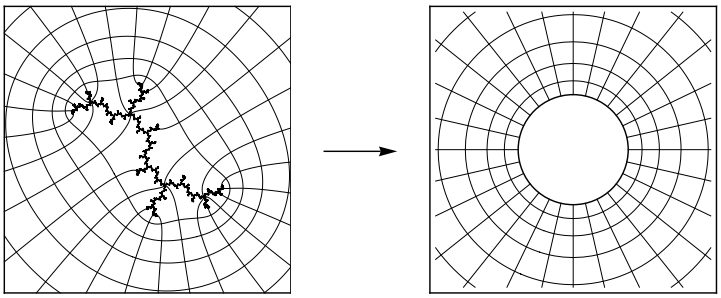

Figure 2.2.1: The Böttcher Map for the dendrite.

2.2 External Rays for the Dendrite

In the same way as described in Chapter 1, there exist a Böttcher map and Caratheadory Loop for the dendrite, shown in Figure 2.2.1. Again, in the same manner as before, we can use the images of radial lines to form external rays for the dendrite. Some external rays for the dendrite are shown in Figure 2.2.2 (a). We will use the external rays to give some more rigorous meaning to the objects and patterns discussed in the previous section.

Unlike the Basilica, which has only one kind of pinch point, the dendrite has at least two, and these are the points that are of primary interest for us. Observe that, as we see in Figure 2.2.2 (b), the main triple point has external rays at 1/7, at 2/7, and at 4/7, and the central pool has external rays at 1/12 and 7/12.

It turns out that it is actually non-trivial that the external rays for the dendrite actually land on the points we expect them to land on. In fact, the rays for the main triple point, $\{1/7, 2/7, 4/7\}$, rather than just touching down directly, form an infinite logarithmic spiral around the point before reaching it. Fortunately, the following theorem of Milnor guarantees that they will land.

Theorem 2.2.1. *(Theorem* 18.3 *of* [7]*) For any given f with connected Julia set, the following are equivalent.*

- *The Julia set ∂J is locally connected.*

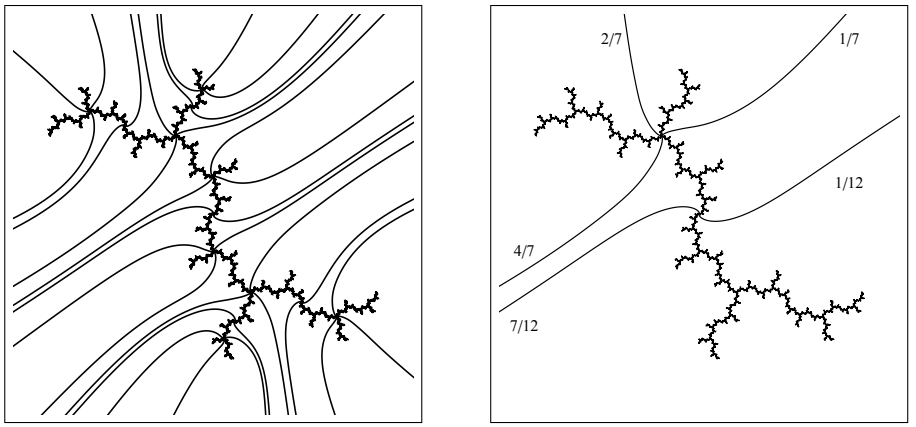

(a) (b)

Figure 2.2.2: (a) Some of the external rays for the dendrite. (b) The external rays for the main triple point and central pool.

- *Every exernal ray R_t lands at a point $\gamma(t)$ which depends continuously on the angle t.*

Because, as we saw in the previous chapter, the fact that the dendrite map is post-critically finite implies that the dendrite is locally connected, we now know that all the external rays do, in fact land, and land where we expect them to land.

Definition 2.2.2. The point located at $z = \frac{1}{2}(1 - \sqrt{1-4i})$, is fixed under the mapping $z^2 + i$, and and has external rays 1/7, 2/7, 4/7. This point we will denote A, and also refer to as the **main triple point** or the **fixed point**.

Definition 2.2.3. The point located at $z = 0$, which has external rays 1/12 and 7/12, we will denote P, and also refer to as the **central pool**.

We will use the external rays to give definitions of pools and triple points in generality.

Definition 2.2.4. A point in the dendrite is called a **triple point** if its removal separates the dendrite into three connected components. Such a point is the landing point for three external rays, whose angles all have of the form

$$\frac{k}{7 \cdot 2^n}$$

for some $k, n \in \mathbb{N}$, where k is congruent to 1, 2 or 4, mod 7.

It turns out that every triple point also has the property that its image under ϕ^m for some finite m is the main triple point, A. Because of this, we know that every external angle of a triple point is eventually mapped to 4/7 under repeated doubling mod 1. Additionally, we know that every ray with an angle of the form $\frac{k}{7 \cdot 2^n}$ where $k \equiv 1$, 2, or 4 mod 7 hits a triple point, but the pattern of which rays hit the same triple points is complicated and we have not found a good characterization for it.

Definition 2.2.5. A point in the dendrite is called a **pool** if it is the landing point for two external rays, both of whose angles are of the form

$$\frac{k}{12 \cdot 2^n}$$

for some $k, n \in \mathbb{N}$, where $k \equiv 1 \mod 6$.

Similarly to the triple points, every pool has the property that its image under ϕ^m for some finite m is the central pool, P. Having established this, we can see that the triple points and the pools are quantifiably different in a way that no two pinch points on the Basilica are. Aside from the obvious fact that they have different numbers of external rays, the angles of those rays ensure that no triple point will ever be mapped to a pool under ϕ, and vice versa. Because the dendrite has no interior, there are in fact uncountably many other pinch points that are neither triple points nor pools. In the context of this project, however, we are only concerned with pinch points that are triple points or pools.

We now use the external rays to reexamine some of the patterns discussed in the previous section. First we will make rigorous the notions of branch arms and dominant triple points for such. First we must give a definition of arms in generality.

Definition 2.2.6. Let R be a triple point, and let $[a, b]$ be an interval bounded by two external rays of R. If the third external ray of R does not lie in $[a, b]$, then $[a, b]$ is an **arm** of R.

Definition 2.2.7. Let $[a, b]$ be an arm. Then $[a, b]$ is a **branch arm** if there exists some $n \in \mathbb{N}$ so that ϕ^n is injective on $[a, b]$ and $\phi^n([a, b])$ is equal to the arm $[4/7, 8/7]$.

Definition 2.2.8. Let $[a, b]$ be an arm. Then if the triple points with angles

$$a + \frac{b-a}{8} \qquad \text{and} \qquad a + \frac{3(b-a)}{8} \qquad \text{and} \qquad a + \frac{7(b-a)}{8}$$

all land at the same point, then that point is the **dominant triple point** for $[a, b]$.

Now consider the section of the dendrite located between the main triple point and the lower triple point. This region is partitioned by the upward facing and downward facing arms of the triple points in the second image of Figure 2.1.2. In Figure 2.2.3 we have the external rays marked for the main triple point, the lower triple point, and the two triple points of interest in between them. Observe that the intervals $[1/14, 1/7]$ and $[4/7, 9/14]$, which correspond to the top and bottom sides of the center section of the dendrite, are partitioned by the external rays for the two interior triple points. In particular, the top section is divided into the intervals $[1/14, 9/112]$, $[9/112, 11/112]$, $[11/112, 15/112]$ and $[15/112, 1/7]$, which are of lengths 1/8, 1/4, 1/2, and 1/8 of the original interval. The same is true of the partition of $[4/9, 9/14]$ by the external rays on the bottom of the center section. In fact, this pattern, of partitioning the interval between two triple points into subintervals of lengths 1/8, 1/4, 1/2, and 1/8 of the original interval, holds in many places throughout the dendrite: whenever the interval along one side of the dendrite between two triple points is the same length as the interval along the other side, this pattern will hold.

Example 2.2.9. Consider the inner two triple points marked in 2.2.3, which have external rays at $\{9/112, 67/112, 71/112\}$ and $\{11/112, 15/112, 65/112\}$. The top interval between these points is $[9/112, 11/112]$, which has length 1/56, and the bottom interval is $[65/112, 67/112]$, which also has length 1/56. If we partition each of these intervals into lengths $1/56 \cdot 1/8 = 1/448$, $1/56 \cdot 1/4 = 1/224$, $1/56 \cdot 1/2 = 1/112$ and 1/448, we break the top interval into $[9/112, 37/448]$, $[37/448, 39/448]$, $[39/448, 43/448]$, and $[43/448, 11/112]$,

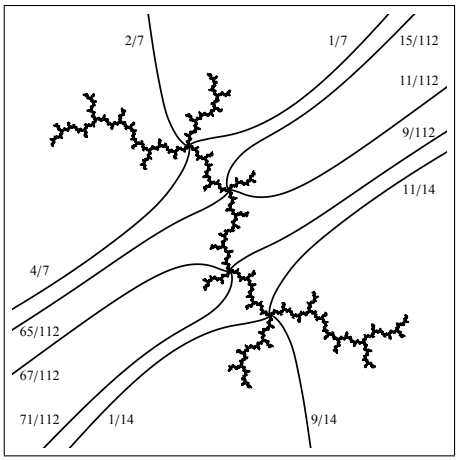

Figure 2.2.3: The external rays for the main triple point, lower triple point and two points of interest.

and we break the bottom interval into $[65/112, 261/448]$, $[261/448, 263/448]$, $[263/448, 267/448]$, $[267/448, 67/112]$. Marking these external rays in Figure 2.2.4, we can see that these clearly correspond to the one-up, one-down triple points that partition the region between the triple points we chose. Any definition we will establish of a segment will have to agree with the notion that this section of the dendrite is a segment.

Now consider the triple points marked in Figure 2.2.4, with external rays at $\{9/56, 11/56, 15/56\}$ and $\{9/28, 11/28, 15/28\}$. The first interval between these points is the interval $[15/56, 9/28]$, which has length $3/56$, and the second is $[15/28, 65/56]$, which has length $5/8$ (noting that we use $65/56$, rather than $9/56$ here, because we want the interval to be continuous; the two are equivalent mod 1). If we partition the first interval into lengths $3/56 \cdot 1/8 = 3/448$, $3/56 \cdot 1/4 = 3/224$, $3/56 \cdot 1/2 = 3/112$ and $3/448$, we have the subintervals $[15/56, 123/448]$, $[123/448, 129/448]$, $[129/448, 141/448]$ and $[141/448, 9/28]$. Then, if we partition the second interval into lengths $5/8 \cdot 1/8 = 5/64$, $5/8 \cdot 1/4 = 5/32$, $5/8 \cdot 1/2 = 5/16$ and $5/64$, we get the subintervals $[15/28, 275/448]$, $[275/448, 345/448]$, $[345/448, 485/448]$, and $[485/448, 65/56]$. Marking these external rays in Figure 2.2.4, we see that they do not conform to any obvious pattern, and certainly do not mark the posi-

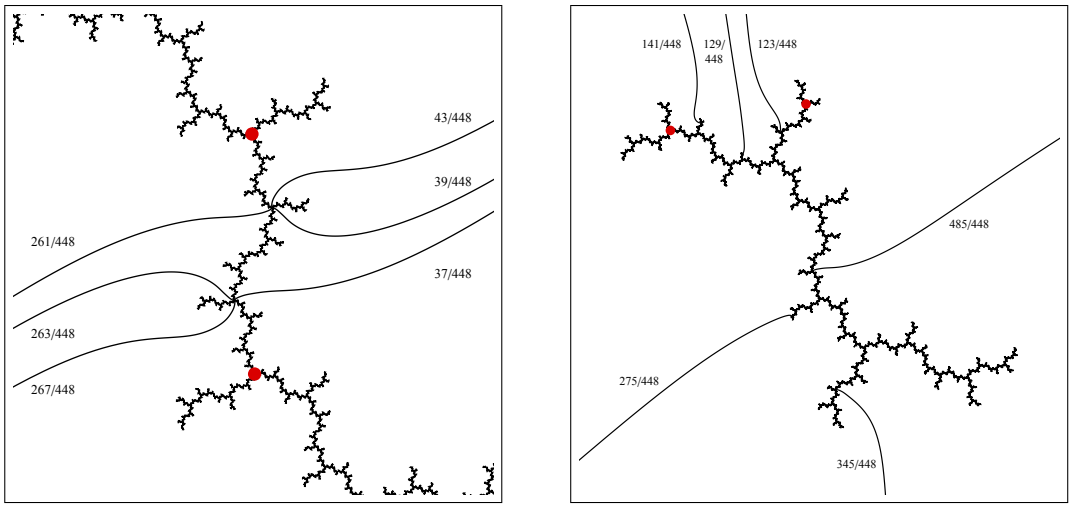

(a) (b)

Figure 2.2.4: (a) These external rays correspond to two triple points partitioning this region. (b) Points for which the pattern does not hold and the external rays between them.

tions of two triple points along the path between the points we began with. Any definition of a segment we may establish must conform to the fact that this is not a segment.

We will now make rigorous the notion of segments and the dominant pools for such.

Definition 2.2.10. Let S be a connected subset of the dendrite that is bounded on one end by a triple point and on the other end by a pool. If for some $n \in \mathbb{N}$ ϕ^n is injective on S and $\phi^n(S)$ is the arm $[4/7, 8/7]$, then S is a **half segment**.

For example, the section of the dendrite bounded by the triple point $\{11/112, 15/112, 65/112\}$ and the central pool is mapped injectively by ϕ to the right-side branch arm of the dominant triple point for the upward-facing arm of the main triple point; since that arm is mapped injectively to $[4/7, 8/7]$ by ϕ^4, then ϕ^5 maps this section injectively to $[4/7, 8/7]$. Thus, the section of the dendrite between the central pool and the triple point $\{11/112, 15/112, 65/112\}$ is a half segment.

Definition 2.2.11. Let S be a connected subset of the dendrite that is bounded on both ends by triple points. If S is the union of two half segments, whose intersection is a pool, and there exists some $n \in \mathbb{N}$ so that each half segment is mapped injectively to $[4/7, 8/7]$ by ϕ^n, then S is a **segment**.

Definition 2.2.12. Let S be a segment. Then the pool that is the intersection of the two half segments that comprise S is called the **dominant pool** for S.

Proposition 2.2.13. *Let S be a segment, and let $n \in \mathbb{N}$ so that ϕ^n maps each half segment of S injectively to $[4/7, 8/7]$. Then the preimages of the lower triple point that lie in each half segment of S partition S into three smaller segments. We call this a **basic partition** of S.*

Proof. Let H be one of the half segments of S, and let H_A be the preimage of the lower triple point in H. Since ϕ^n maps H injectively to $[4/7, 8/7]$, the section of H between H_A and the dominant pool of S is mapped to the branch arm $[9/14, 11/14]$ by ϕ^n. Thus, since that arm is mapped injectively to $[4/7, 8/7]$ by ϕ^3, we see that the section of H between H_A and the dominant pool is mapped injectively to $[4/7, 8/7]$ by ϕ^{n+3}. The same argument holds for the corresponding piece of the other half segment of S; thus, both pieces share the dominant pool of S and map to $[4/7, 8/7]$, so their union is a segment.

Now consider the piece of H between H_A and the triple point that is the other end of H. Since ϕ^n maps H injectively to $[4/7, 8/7]$, that section is mapped to the segment bounded by the main triple point and the lower triple point. Since both half-segments of that segment are mapped to $[4/7, 8/7]$ by ϕ^3, we see that ϕ^{n+3} maps both halves of this piece of H injectively to $[4/7, 8/7]$; thus, it is a segment, and the result is proven. □

Proposition 2.2.14. *Every branch arm has a dominant triple point, which partitions it into two branch arms and a segment.*

Proof. Let $[a, b]$ be a branch arm. Then, as in the previous lemma, we note that there is some $n \in \mathbb{N}$ so that ϕ^n is injective on $[a, b]$ and $\phi^n([a, b]) = [4/7, 8/7]$. Then, as before, we see that $[a, b]$ has the same structure as $[4/7, 8/7]$, so if A' is the lower triple point, then $(\phi^n)^{-1}(A')$ is a dominant triple point for $[a, b]$.

To show that the two arms of the dominant triple point are branch arms, note that the arms of A' are also branch arms; $[9/14, 11/14]$ maps injectively to $[4/7, 8/7]$ under ϕ^2, and $[11/14, 15/14]$ maps injectively to $[4/7, 8/7]$ under ϕ. Thus, if $[c, d]$ and $[h, k]$ are the arms of the dominant triple point of $[a, b]$, and $\phi^n([c, d]) = [9/14, 11/14]$, we see that $\phi^{n+2}([c, d]) = [4/7, 8/7]$, and similarly, $\phi^{n+1}([h, k]) = [4/7, 8/7]$, so both $[c, d]$ and $[h, k]$ are branch arms.

To show that the third piece of $[a, b]$ is a segment is essentially trivial; since $[a, b]$ maps injectively to $[4/7, 8/7]$ under ϕ^n, the third piece maps injectively to the central segment under ϕ^n; as we saw in the proof of the previous proposition, this implies that the piece is a segment. □

From this proof, we obtain an easy corollary.

Corollary 2.2.15. *There are infinitely many branch arms and segments in the dendrite.*

The final result of this section will be to use the external angles to show that the triple points and pools are dense in the dendrite.

Proposition 2.2.16. *The triple points and pools are dense in the dendrite.*

Proof. It will suffice to show that the external angles of the triple points and pools are dense in the interval $[0, 1]$, since if a point has external angles that lie between those of two other points, then that point lies between the other two. We will here show that the triple points are dense; the proof for the pools is analogous. Let $a, b \in [0, 1]$, and suppose that $a < b$. Then the interval $[a, b]$ has length $b - a$. Recall that the external angles for

triple points have the form

$$\frac{k}{7 \cdot 2^n}$$

for some $n, k \in \mathbb{Z}$, so that $k \cong 1$, 2, or 7 mod n. In particular, we will consider fractions of the form

$$\frac{7k+2}{7 \cdot 2^n}.$$

We verify that this must be a triple point external angle, since after n doublings, we obtain

$$\frac{7k+2}{7} \equiv \frac{2}{7} \mod 1.$$

Then we consider an interval of the form $[\frac{k}{2^n}, \frac{2k}{2^n}]$, which has length $k/2^n$. Because k and n are arbitrary, we can choose them so that $k/2^n < (b-a)/3$, so there must be an entire such interval contained in $[a, b]$. But see that this interval is equivalent to $[\frac{7k}{7 \cdot 2^n}, \frac{14k}{7 \cdot 2^n}]$. Then note that for any $k \in \mathbb{N}$, $7k < 7k+2 < 8k$. Therefore, there must be some rational number of the form

$$\frac{7k+2}{7 \cdot 2^n}$$

contained in $[\frac{7k}{7 \cdot 2^n}, \frac{14k}{7 \cdot 2^n}] \subseteq [a, b]$, thus proving the claim.

□

2.3 The Dendrite Lamination

As with the Basilica, we want to construct an invariant lamination for the dendrite, which we will go on to use in the construction of our group. Unlike the Basilica, though, which has only one kind of pinch point, and for which there are gaps between arcs in the lamination, the dendrite has uncountably many pinch points, and we will see that the arcs of the dendrite lamination have a subspaces homeomorphic to $C \times [0, 1]$, where C is a Cantor set. As we said before, though, we will not consider every pinch point of the dendrite; we are only interested in pinch points that are triple points or pools, and we will construct a lamination accordingly.

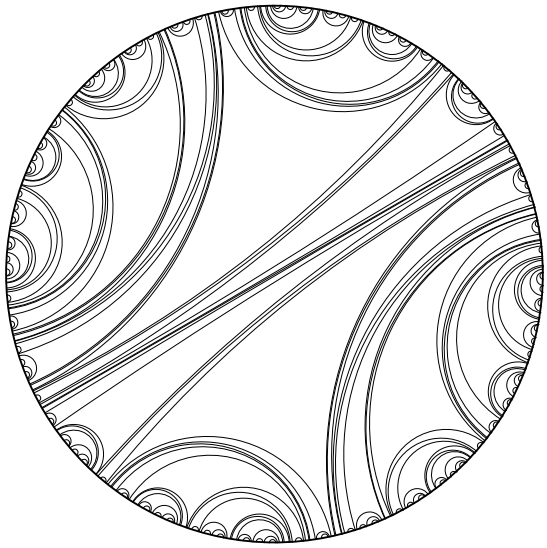

Figure 2.3.1: The invariant lamination for the dendrite.

We begin with the unit circle, and, as before, add arcs connecting any two points on the circle for which the external rays land at the same point, if that point is either a triple point or a pool. Thus, we connect the points 1/7, 2/7 and 4/7 in a triangle, and we connect the points 1/12 and 7/12 in an arc.

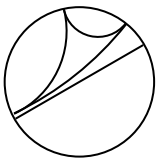

We continue in this manner, drawing more triangles for the triple points, and more arcs for the pools.

We refer to the arc that corresponds to the central pool as the **central pool arc**, and the triangle that corresponds to the main triple point as the **main triangle**; other names are obtained in a similar fashion. Note that in general, when we speak of arcs, or objects in

the lamination, a triangle is counted as only one arc, or object in the lamination, since it corresponds to just one point, even though it is comprised of three actual arcs. Though we have drawn all of the triple point arcs and pool arcs, this is not the complete lamination, however, since there are in fact uncountably many other pinch points on the dendrite. It turns out that the arcs that we have obtained form a Cantor set in the lamination, and because the triple points and pools are dense in the dendrite and in the lamination, the closure of that set forms the set of all pinch points in the dendrite. Hence, we obtain the invariant lamination for the dendrite by adding the arcs for those additional points, seen in Figure 2.3.1.

2.4 The Ancestry Partial Order

In this section, we develop an important notion that will allow us to prove a number of results about the dendrite. Much of what we intend to do rests upon the ability to make quantifiable statements about the relative "sizes" of points in the dendrite. To that end, we will develop a partial order on the set of all triple points and pools that is designed to agree with some intuitive notions about such size. We will begin with a brief informal discussion of what such a partial order should do.

The first thing that we want the partial order to do is conform to some intuitive notion of size for triple points. This is easier to discern than for pools, because triple points have arms, and we can simply compare the size of the arms. Obviously, this does not work as a real computational tool, since for any triple point, the external rays simply partition the unit circle into three pieces, and the sum of the lengths of the pieces is always one. Nonetheless, it seems as though it should be true that the main triple point is "larger" than the triple point with external rays $\{9/56, 11/56, 15/56\}$, both of which are marked in the left of Figure 2.4.1. It also seems reasonable that we should require the main triple

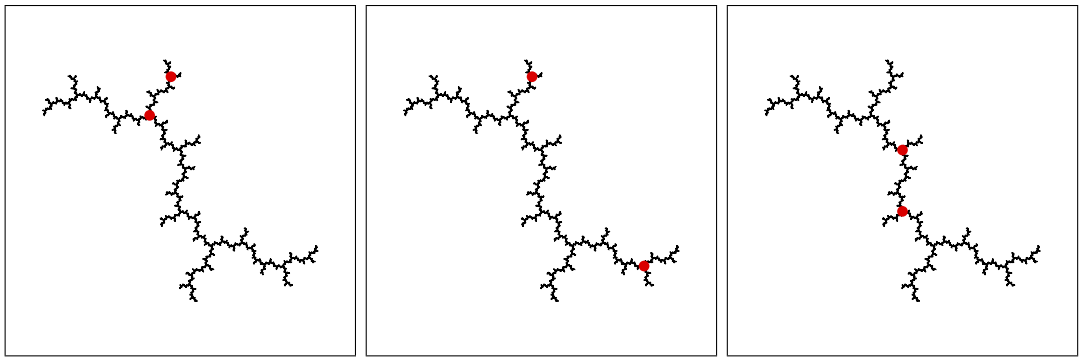

Figure 2.4.1: Left: Two triple points. Center: Two unrelated triple points. Right: The children of the central pool.

point to be larger than any other point, even though the arms attached to the lower triple point are the same sizes as those attached to the main triple point.

In general, we might define the relation as being that $A \preceq B$ when the denominators for the external rays of A are smaller than those for B. This is a good rule, but it is not quite the one we want to use. In particular, this would require that we define the relation between the two points marked in the center of Figure 2.4.1, which, though certainly possible, we don't want to do. In particular, we want the relation to represent the branching of the dendrite, and as such, we want it to be defined such that each point has 'children', which are the points that branch off from it. In this sense, the points marked in the center of Figure 2.4.1 should not be comparable, since they lie on different arms of the main triple point. Because we wish to have our relation correspond to this notion of ancestry, we will find it convenient to define it recursively, rather than absolutely.

The other thing to mention is that we want to say something about the position of the pools in this relation. We determined that the central pool should be the child of the lower triple point, and that the two points marked in the right of Figure 2.4.1 should be the children of the central pool. Repeated on all similar structures in the dendrite, these patterns will be sufficient to define the relation we want.

We are now ready to begin defining our relation. Every triple point has three children, and every pool has two. Where the external rays for a point partition the unit circle into either two or three pieces, the point has one child in each segment of the circle.

Definition 2.4.1. Let P and Q each be a triple point or pool. Then P is an ancestor of Q if either

1. Q lies in a branch arm of P.
2. Q lies in a segment having P as an endpoint.
3. Q lies in a segment for which P is the dominant pool.

Definition 2.4.2. Let P and Q each be a triple point or pool. Then P is the **parent** of Q, and Q is a **child** of P, if P is an ancestor of Q, and every other ancestor of Q is also an ancestor of P.

We now verify that this partial order satisfies the conditions we set for it at the beginning of the section. It is clear from the definition that this partial order begins with the main triple point and branches outward thence. We see in the first image of Figure 2.4.2 the main triple point marked in red, and its children marked in blue. In the second image, we have added the grandchildren of the main triple point in green, and in the third image, we have added the great-grandchildren of the main triple point in yellow. We will make extensive use of this partial order, both to define our piecewise-linear homeomorphisms of the dendrite, and to prove important results about the group we will define in the next chapter.

2.5 Finite Arc Diagrams

In this section, we will use the ancestry relation to identify subsets of the lamination called **finite arc diagrams**. As with Belk and Forrest, we will then use these finite arc

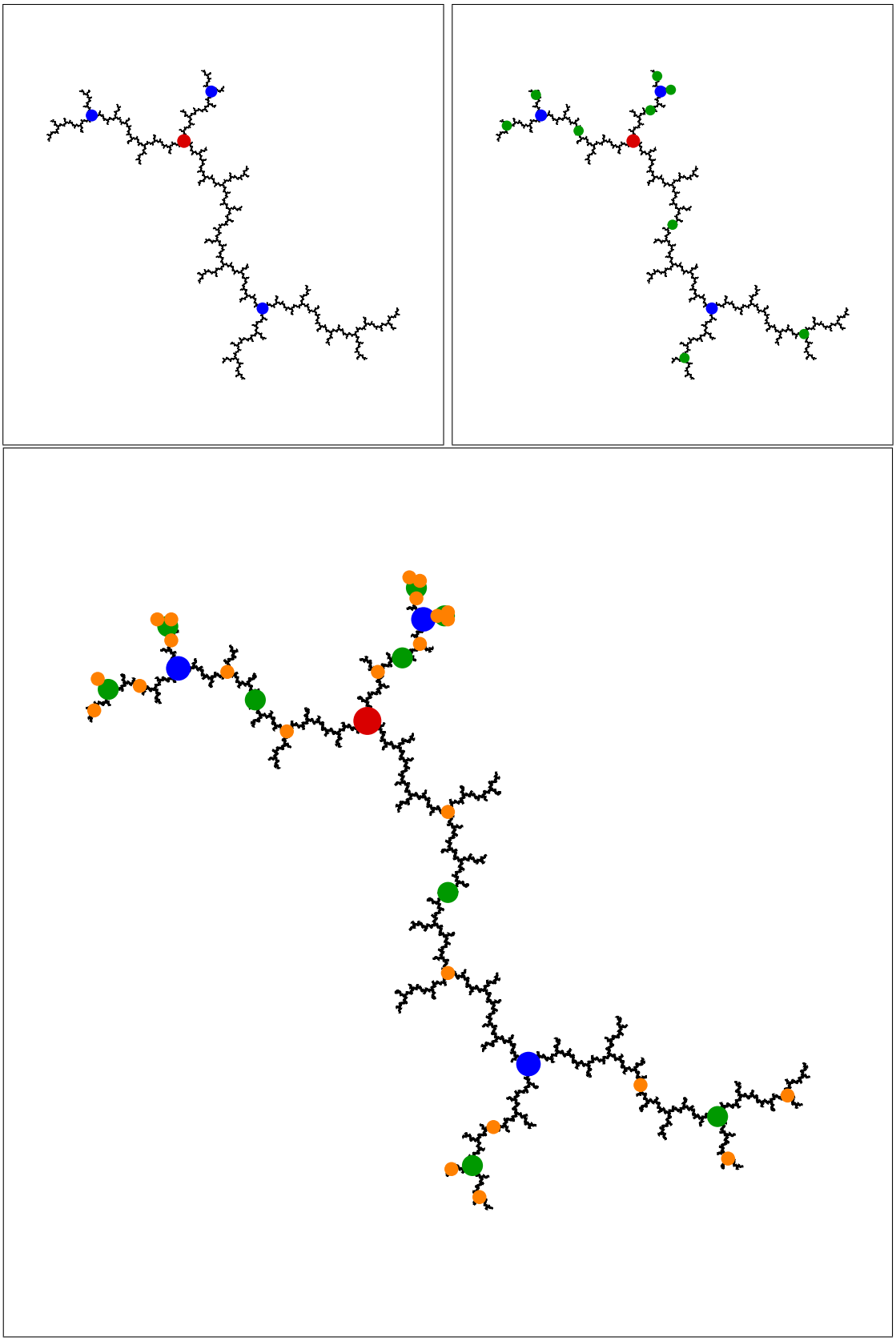

Figure 2.4.2: The main triple point, its children, its grandchildren, and its great-grandchildren.

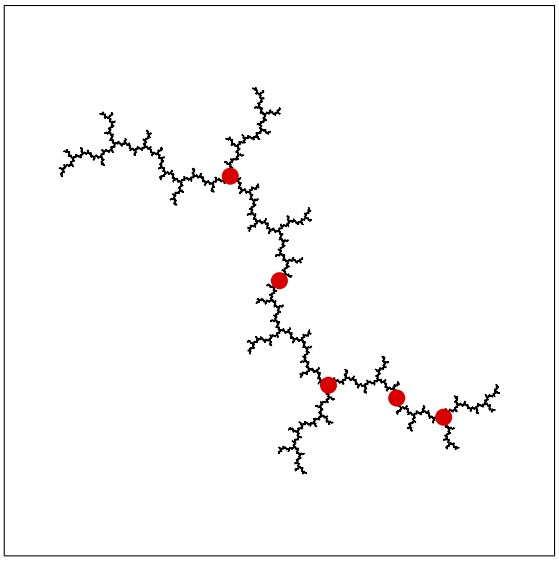

Figure 2.5.1: The points corresponding to the arcs in Example 2.5.3.

diagrams to define certain allowable mappings of the lamination to itself, and find that those mappings descend to mappings of the dendrite, which will be the focus of this work. Much of the work has already been laid out at this point, though; having already constructed ancestry, construction of finite arc diagrams is very easy. Note that, while the ancestry relation is defined on triple points and pools in the dendrite, we often speak of it as applying to objects in the lamination as well.

Definition 2.5.1. Let R and S each be a triple point triangle or a pool arc in the lamination, and let R' and S' be the points in the dendrite they correspond to. If R' is an ancestor of S', then we say R is an ancestor of S.

We now define finite arc diagram.

Definition 2.5.2. Let F be a finite set of triple point arcs and pool arcs in the dendrite lamination. If for each $A \in F$, every ancestor of A is also contained in F, then the diagram constructed by drawing all the arcs in F in the unit circle is a **finite arc diagram**.

We now give a simple example of a finite arc diagram.

Example 2.5.3. Consider the following subset of the lamination

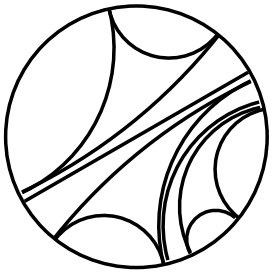

which has arcs corresponding to the main triple point, the lower triple point, the central pool, the triple point $\{1/28, 23/28, 25/28\}$ and the pool $\{1/24, 19/24\}$, which are marked in Figure 2.5.1. First, observe that the main triple point has no ancestors, so consequently, its triangle has no ancestors, and thus, all of the ancestors of its triangle are included. Then see that the lower triple point lies in the branch arm $[4/7, 8/7]$ of the main triple point, but does not lie in any other branch arms or segments, so its only ancestor is the main triple point. Thus, all the ancestors of the the triangle corresponding to the lower triple point are included. Because the central pool lies in the same branch arm of the main triple point, and also lies in the segment bounded by the main triple point and the lower triple point, and in no other branch arms or segments, we see that the only ancestors of the central pool arc are the main and lower triple point triangles, which are included. In a similar fashion, we see that the ancestors of the triple point $\{1/28, 23/28, 25/28\}$ are the lower triple point and the main triple point, and the ancestors of the pool $\{1/24, 19/24\}$ are that triple point, the lower triple point, and the main triple point. Therefore, all the ancestors of every object in this finite subset of the lamination are included, so this is indeed a finite arc diagram.

We can now use these finite arc diagrams to define maps from the lamination to itself. In the manner of Belk and Forrest, we can think of any finite arc diagram as a 2-complex, with the arcs and intervals as edges, and the regions between them as faces. We say that two

finite arc diagrams are **isomorphic** if there exists an orientation-preserving isomorphism between the corresponding complexes.

We can see that any finite arc diagram partitions the unit circle into intervals with endpoints that are external angles for triple points or pools. Given an isomorphism $\phi : \mathcal{D} \longrightarrow \mathcal{R}$ between two finite arc diagrams, we can define a piecewise-linear homeomorphism of the circle by simply mapping each such interval of the domain linearly to the corresponding interval of the range. Because the interiors of triangles must always be mapped to the interiors of triangles by virtue of having three edges and the spaces between elements of an arc diagram must be mapped to other such spaces, by virtue of having four edges, we can see that breakpoints corresponding to triple point external angles in $\mathcal{D}$ must be mapped to the same in $\mathcal{R}$, and breakpoints corresponding to pool external angles in $\mathcal{D}$ must also be mapped to the same in $\mathcal{R}$. Because of this, we find that such a homeomorphism preserves the dendrite lamination, and consequently, descends to a self-homeomorphism of the dendrite, as follows.

Recall that a Julia set, ∂J is a quotient of the circle, S^1 under ψ, the Caratheodory loop. Then if f is a mapping from the circle to itself, we can construct the following diagram:

$$\begin{array}{ccc} S^1 & \xrightarrow{f} & S^1 \\ {\scriptstyle\psi}\downarrow & & \downarrow{\scriptstyle\psi} \\ \partial J & & \partial J. \end{array}$$

To complete the diagram, we construct a function $g : \partial J \longrightarrow \partial J$ so that $g \circ \psi = \psi \circ f$. Because ψ is not injective, require another condition on f, which is that if $\psi(\theta) = \psi(\phi)$, then $\psi(f(\theta)) = \psi(f(\phi))$ for $\theta, \phi \in [0, 1]$. Additionally, we want f and g to both be continuous and bijective. Because ψ is a quotient map, if f is continuous, g must also be continuous. To ensure that f and g are bijective, we need them to be invertible, so we must strengthen our previous condition to require that $\psi(\theta) = \psi(\phi)$ if and only if

$\psi(f(\theta)) = \psi(f(\phi))$. Then we can complete the diagram and give a definition.

$$\begin{array}{ccc} S^1 & \xrightarrow{f} & S^1 \\ {\scriptstyle\psi}\downarrow & & \downarrow{\scriptstyle\psi} \\ \partial J & \xrightarrow{g} & \partial J. \end{array}$$

Definition 2.5.4. A **dyadic rearrangment of a Julia set**, $g : \partial J \to \partial J$, is the image under ψ of a piecewise-linear homeomorphism of the circle $f : S^1 \to S^1$ such that for $\theta, \phi \in [0, 1]$, $\psi(\theta) = \psi(\phi)$ if and only if $\psi(f(\theta)) = \psi(f(\phi))$, and the breakpoints of f correspond to triple points and pools.

This is equivalent to saying that a dyadic rearrangement is the image under ψ of a piecewise-linear homeomorphism of the circle obtained by an isomorphism of finite arc diagrams, since such a mapping must preserve the dendrite lamination in the same way that an isomorphism must.

In a more intuitive way, we can define dyadic rearrangments the dendrite by giving a piecewise-linear definition of a function on the external angles of the Julia set. Because we specify that $\psi(\theta) = \psi(\phi)$ if and only if $\psi(f(\theta)) = \psi(f(\phi))$, we thus ensure that the function "works"; that is, that we map triple-points to triple-points and pools to pools, and otherwise preserve the local structure of the dendrite. Note that in [1], Belk and Forrest chose the term 'dyadic rearrangement' because the piecewise-linear homeomorphism descending to a map on the Basilica had breakpoints at the dyadic points of the circle; here we simply use the term as a convenience to agree with their notation. We now give an example of such a mapping.

Example 2.5.5. In Figure 2.5.2, we see an isomorphic pair of finite arc diagrams, which in turn induce a rearrangement of the dendrite. We refer to such a picture as an **arc pair diagram**. Note that we must mark a corresponding pair of points to specify the mapping; otherwise rotations might be allowed. This picture gives the following piecewise-linear homeomorphism of the circle

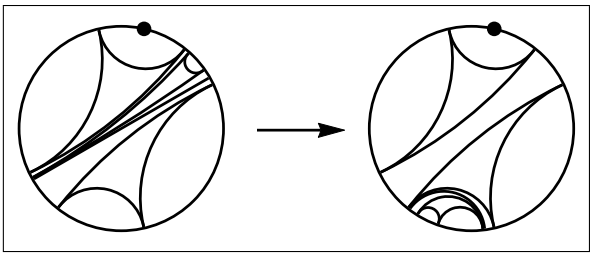

Figure 2.5.2: An isomorphic pair of finite arc diagrams.

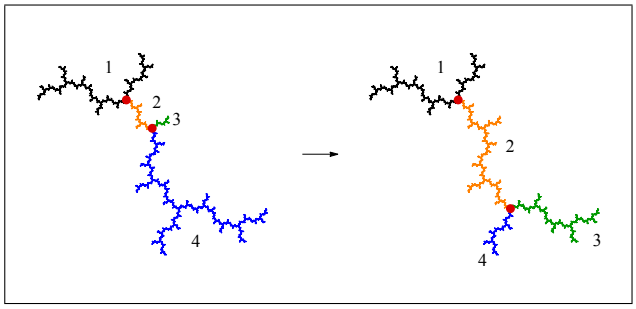

Figure 2.5.3: The action of γ on the dendrite.

$$\gamma(\theta) = \begin{cases} \theta + 11/16 & \text{if } 1/12 \leq \theta \leq 11/112 \\ 8\theta & \text{if } 11/112 \leq \theta \leq 1/7 \\ \theta & \text{if } 1/7 \leq \theta \leq 4/7 \\ 8\theta & \text{if } 4/7 \leq \theta \leq 65/112 \\ \theta + 1/16 & \text{if } 65/112 \leq \theta \leq 7/12 \\ 1/4\theta + 1/16 & \text{if } 7/12 \leq \theta \leq 13/12 \end{cases}$$

which descends to the mapping of the dendrite shown in Figure 2.5.3.

A final thing to note is that, while every dyadic rearrangement of the dendrite has an arc pair diagram, it is not the case that the arc pair diagram will be unique. For example, in the function considered above, we may add the pool arc for the point $\{13/96, 55/96\}$ to the domain picture, and its image under the mapping, which is the central pool arc, to the range picture, and have the same function resultant, shown in Figure 2.5.4.

Definition 2.5.6. An **expansion** of an arc pair diagram consists of adding a object to the domain arc diagram, all of whose ancestors are already included, and adding the image of that object to the range arc diagram.

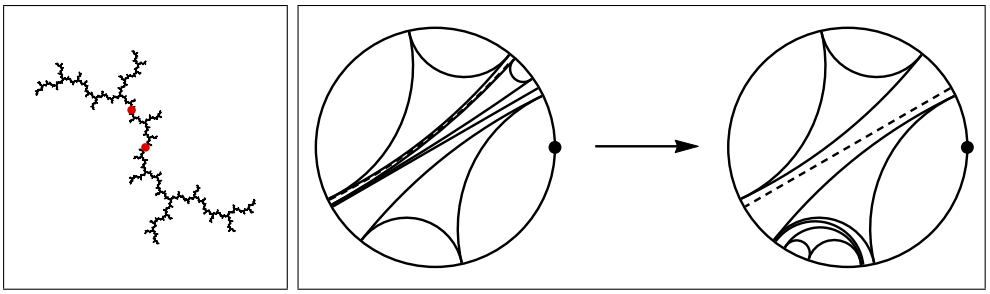

Figure 2.5.4: Arcs added to the arc pair diagram for γ.

Definition 2.5.7. A **reduction** of an arc pair diagram is the inverse of an expansion.

An arc pair diagram is said to be **reduced** if no reductions are possible. Belk and Forrest prove the following proposition in [1] for the Basilica; we present an adaptation of their proof.

Proposition 2.5.8. *Every dyadic rearrangement of the dendrite has a unique reduced arc pair diagram.*

Proof. Let f be a dyadic rearrangement of the dendrite. Given an interval I with endpoints corresponding to external angles for pools or triple points, we say that I is **regular** if f is linear on I and the image $f(I)$ also has endpoints of the corresponding types. The domain intervals of any arc pair diagram for f must be regular. An arc pair diagram for f is reduced if and only if each of the regular intervals in its domain is maximal under inclusion.

If the interiors of any two regular intervals have nontrivial intersection, then it must be the case that f has the same slope on both of them, since f has the same slope everywhere inside each one, and it must agree on the overlap. Thus if the interiors of two regular intervals have nontrivial intersection, then their union is also regular, so neither of them is maximal. Hence, any two maximal regular intervals have disjoint interiors, so there can only be one partition of the circle into maximal regular intervals. □

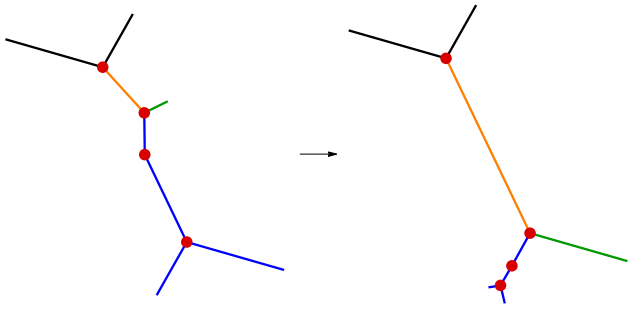

Figure 2.6.1: A finite tree diagram for γ.

2.6 Finite Subtrees and Finite Tree Diagrams

Although dyadic rearrangements of the dendrite are defined in terms of isomorphic finite arc diagrams, we often in practice use a different kind of picture to work with them. These are called **finite tree diagrams** for such functions, and make use of the tree-like structure of the dendrite. We first define a **finite subtree** of the dendrite, and then give the desired definition.

Definition 2.6.1. Let S be a finite arc diagram of the dendrite. A **finite subtree** of the dendrite corresponding to S is a graph that contains one vertex for each object in S; vertices are connected if there is a path between the corresponding objets in S that does not cross any other arcs, and the vertices corresponding to the main triple point and the central pool are marked.

Definition 2.6.2. Let f be a piecewise-linear function acting on the dendrite. Then the **finite tree diagram** for f consists of two finite subtrees of the dendrite that correspond to the domain and range pieces of the finite arc diagram for f.

Because there is an exact correspondence between the vertices of a finite subtree and the objects in a finite arc diagram, it is clear that each one uniquely determines the other. Recalling the example of a dyadic rearrangement of the dendrite given in the previous section, we show in Figure 2.6.1 a finite tree diagram for γ.

Observe that this diagram contains all the same information that the arc pair diagram does, since all the points whose objects are represented in the arc pair diagram are marked, and the combination of their positioning and the coloring of the diagram makes it clear that no rotation has occurred.

3
The Group T_D

3.1 The Group T_D

Definition 3.1.1. The set $\boldsymbol{T_D}$ is the set of all dyadic rearrangements of the dendrite.

We will show that T_D forms a group under composition.

Theorem 3.1.2. *Let f be a piecewise-linear homeomorphism of the circle. Then f induces a dyadic rearrangement of the dendrite if and only if it satisfies the following conditions.*

1. *The dendrite lamination is invariant under f.*
2. *Every breakpoint of f is the endpoint of a triple point arc or pool arc in the lamination.*

In particular, T_D forms a group under composition.

Proof. The forward definition follows immediately from the definition of a dyadic rearrangement of the dendrite. To show the converse, let D be the partition of the unit circle determined by the breakpoints of f, and let R be the partition of the unit circle determined by the images of those points under f. Then let D' and R' be the sets of all objects

in the dendrite lamination that have endpoints at elements of D and R, respectively. Then let $\mathcal{D}$ be the union of D' with the set of all ancestors of elements of D' and the set of the preimages of all the ancestors of elements of R', and let $\mathcal{R}$ be the union of R' with the set of all ancestors of elements of R' and the set of the images of all the ancestors of elements of D'. Then it is clear that f is linear on the partition of the circle determined by the breakpoints of $\mathcal{D}$, and that the partition of the circle determined by the breakpoints of $\mathcal{R}$ is the image of that partition by f. Then we can see that $\mathcal{D}$ and $\mathcal{R}$ are isomorphic, and contain all of their ancestors, so the map $\mathcal{D} \longrightarrow \mathcal{R}$ is an arc pair diagram for f, and hence, f is a dyadic rearrangement of the dendrite. □

We now present an important lemma and corollary that will be essential to the next section.

Let $f, g \in T_D$, and consider the reduced arc pair diagrams for f and g. Let D_f and D_g denote the sets of objects in the domain pieces of reduced finite arc diagrams for f and g respectively, and let R_f and R_g likewise denote the sets of objects in the range pieces of the reduced finite arc diagrams for f and g.

Lemma 3.1.3. *Consider the composition $f \circ g$. Then the set of objects in the domain piece of the reduced arc pair diagram for $f \circ g$ is a subset of $g^{-1}(D_f \cup R_g)$, and the set of objects in the range piece of the same is a subset of $f(D_f \cup R_g)$.*

Proof. Let R be an object in the domain piece of the reduced arc pair diagram for $f \circ g$. Then it must be the case that either $R, g(R)$ cannot be removed from the lamination for g, or $g(R), f(g(R))$ cannot be removed from the lamination for f. If the first is the case, then $g(R) \in R_g$, so $g^{-1}(g(R)) = R \in g^1(D_f \cup R_g)$. If the second is the case, then $g(R) \in D_f$), so the same holds. The second half of the proof is analogous. □

Corollary 3.1.4. *Let m be the number of objects in the reduced finite arc diagram for f, and let n be the number of objects in the reduced finite arc diagram for g. Then if $D_f \cup R_g = D_f$, the number of objects in the diagram for $f \circ g$ is less than or equal to m, and if $D_f \cup R_g = R_g$, the number of objects in the diagram for $f \circ g$ is less than or equal to n.*

Proof. Suppose that $D_f \cup R_g = D_f$. Then by Lemma 3.1.3, it must be the case that $f(D_f) = R_f$ is the set of objects in the range piece of the diagram for $f \circ g$, and $g^{-1}(D_f)$ is the set of objects in the domain piece of the same. It is clear that $|g^{-1}(D_f)| = |D_f|$, and consequently, there are the same number of objects in both the domain and range pictures for $f \circ g$ as in the domain and range pictures for f. Therefore, allowing for the possibility of new allowed reductions, the number of objects in the reduced finite arc diagram for $f \circ g$ is less than or equal to m.

A similar argument will prove the second piece of the claim. □

3.2 Generators for T_D

In this section, we attempt to give a generating set for the group T_D. First, we define some piecewise-linear functions on the dendrite.

Let

$$\alpha(\theta) = \begin{cases} 2\theta & \text{if } 1/7 \leq \theta \leq 4/7 \\ 1/4\theta & \text{if } 4/7 \leq \theta \leq 8/7 \end{cases}$$

$$\beta(\theta) = \begin{cases} 4\theta - 1/112 & \text{if } 1/12 \leq \theta \leq 11/112 \\ 8\theta - 4/7 & \text{if } 11/112 \leq \theta \leq 15/112 \\ 4\theta - 1/4 & \text{if } 11/112 \leq \theta \leq 1/7 \\ 1/2\theta + 1/4 & \text{if } 1/7 \leq \theta \leq 4/7 \\ 4\theta - 1/112 & \text{if } 4/7 \leq \theta \leq 65/112 \\ 8\theta - 4/7 & \text{if } 65/112 \leq \theta \leq 7/12 \\ \theta & \text{if } 7/12 \leq \theta \leq 13/12 \end{cases}$$

$$\delta(\theta) = \theta + 1/2$$

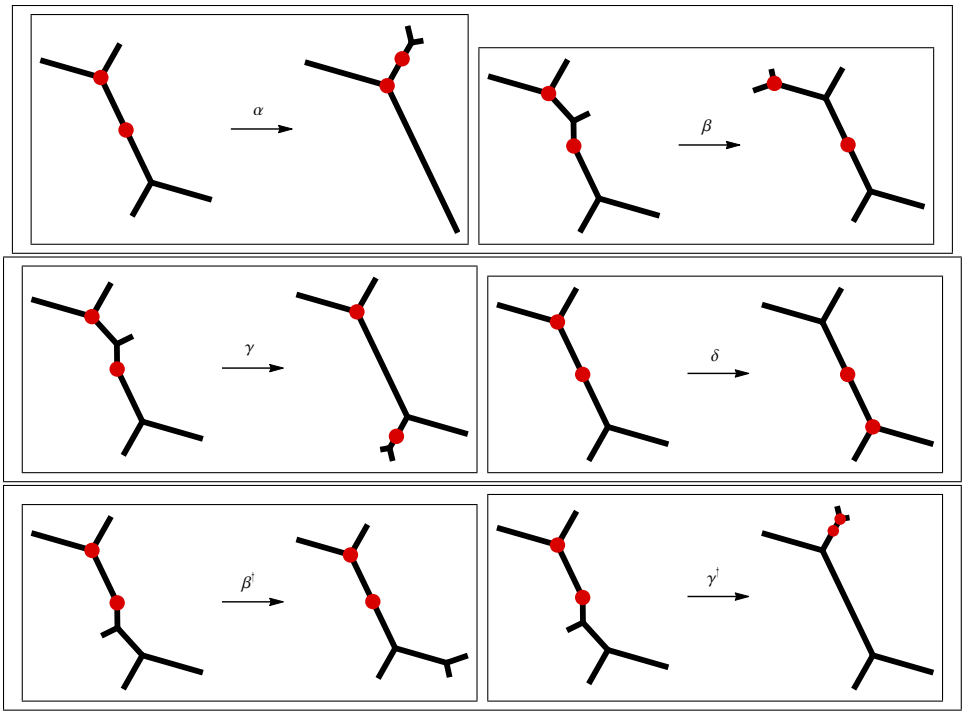

Figure 3.2.1: The Actions of α, β, γ, δ, $\beta^\dagger$, and $\gamma^\dagger$ on the dendrite

We also define some useful elements of $\langle \alpha, \beta, \delta \rangle$. Let

$$\gamma = \delta \circ \alpha \circ \beta$$

$$\beta^\dagger = \delta \circ \beta \circ \delta^{-1}$$

$$\gamma^\dagger = \delta \circ \gamma \circ \delta^{-1}$$

Tree diagrams for of these functions are shown in Figure 3.2.1. We also define some notation here.

Definition 3.2.1. The **left and right children of the central pool**, which we denote P_L and P_R, respectively, are the triple points located at $\{11/112, 15/112, 65/112\}$ and $\{9/112, 67/112, 71/112\}$. We denote the main triple point by A, the central pool by P, and the lower triple point by A'.

Lemma 3.2.2. *Every triple point that lies on the path from A to A' can be mapped to A by an element of $\langle \beta, \gamma, \delta \rangle$.*

Proof. Let R be a triple point that lies on the path from A to A'. Then we know that R has the central pool as an ancestor.

Let n be the number of ancestors of R. Because R has the central pool as an ancestor, we know $n \geq 3$, since the main triangle and the lower main triangle must also be ancestors of R. We proceed by induction on n.

Base case: suppose $n = 3$. In this case, R must be a child of the central pool. If R is equal to P_L, then $\beta(R)$ is equal to the main triangle, and we are done. If R is equal to P_R, then $\gamma^\dagger(R)$ is equal to the main triangle, and we are done.

Now suppose that $n > 3$. Then R is a descendent of either P_L or P_R, and is located either to the left or to the right of its ancestor. So we have four cases.

Case 1: Suppose that R has P_L as an ancestor and is located to the left of P_L. Then we see that $\gamma(P_L) = A'$, and $\gamma(A')$ is not an ancestor of $\gamma(R)$. Thus, $\gamma(R)$ has at most $n - 1$ ancestors.

Case 2: Suppose that R has P_L as an ancestor and is located to the right of P_L. Then we see that $\beta(P_L) = A$, and $\beta(A)$ is not an ancestor of $\beta(R)$. Thus, $\beta(R)$ has at most $n - 1$ ancestors.

Case 3: Suppose that R has P_R as an ancestor and is located to the left of P_R. Then we see that $\beta^\dagger(P_R) = A'$ and $\beta^\dagger(A')$ is not an ancestor of $\beta^\dagger(R)$. Thus, $\beta^\dagger(R)$ has at most $n - 1$ ancestors.

Case 4: Suppose that R has P_R as an ancestor and is located to the right of P_R. Then we see that $\gamma^\dagger(P_R) = A$ and $\gamma^\dagger(A)$ is not an ancestor of $\gamma^\dagger(R)$. Thus, $\gamma^\dagger(R)$ has at most $n - 1$ ancestors.

Therefore, by our inductive hypothesis, in any of these cases, R can be mapped to A by an element of $\langle \beta, \gamma, \delta \rangle$. □

Lemma 3.2.3. *Every triple point in the dendrite can be mapped to A by an element of $\langle \alpha, \beta, \delta \rangle$, and every pool in the dendrite can be mapped to P by an element of $\langle \alpha, \beta, \delta \rangle$.*

Proof. We will begin by making an argument for the triple points, and then make an argument for the pools.

Let R be a triple point, and let n be the number of ancestors of R. We will proceed by induction on n.

If $n = 0$, then R is already equal to A and we are done. Otherwise suppose that $n > 0$. Then we see that R must lie either in the interval $[1/7, 4/7]$, or in the interval $[9/14, 15/14]$ or R must lie between A and A'. So we have three cases.

Case 1: If R lies in $[1/7, 4/7]$, then observe that it is possible to map R into the interval $[4/7, 8/7]$ by either α or α^2 without increasing the number of ancestors of R. Thus, this case can be reduced to one of the other two cases.

Case 2: If R lies in the interval $[9/14, 15/14]$, then observe that under δ, every ancestor up to A' is remains an ancestor of $\delta(R)$, but the image of A under δ, which is A', is not an ancestor of $\delta(R)$, since $\delta(R)$ lies in $[1/7, 4/7]$, and so must not have A' as an ancestor. Thus, $\delta(R)$ has at most $n - 1$ ancestors.

Case 3: If R lies between A and A', then R must have some ancestor, R^* that lies on the path from A to A'. Then by Lemma 3.2.2, there is some $f \in \langle \beta, \gamma, \delta \rangle$ such that $f(R^*) = A$. Then observe that every ancestor of R^*, all of which are ancestors of R as well, must no longer be ancestors of $f(R)$. Thus, because R^* must have had at least three ancestors, $f(R)$ has at most $n - 3$ ancestors.

Therefore, by our induction hypothesis, it follows that in each case, R can be mapped to A by some element of $\langle \alpha, \beta, \delta \rangle$.

Now we will consider pool arcs. Let S be a pool arc, and let n be the number of ancestors of S. We will proceed by induction on n. If $n = 2$, then S is already equal to P, and we are done. Otherwise, suppose that $n > 2$. Consider S^*, the parent of S, and note that S^* has $n-1$ ancestors. Because we know that S^* is a triangle, then by the above, there exists some function μ such that $\mu(S^*)$ has at most $n-2$ ancestors. Thus, $\mu(S)$ has at most $n-1$ ancestors. Then by our induction hypothesis, it follows that $\mu(S)$ can be mapped to P by some element of $\langle \alpha, \beta, \gamma, \delta \rangle$, and therefore, S can as well. □

The following corollary follows immediately from Lemma 3.2.3.

Corollary 3.2.4. *Each triple point in the dendrite can be mapped to each other triple point in the dendrite by an element of $\langle \alpha, \beta, \delta \rangle$, and each pool in the dendrite can be mapped to each other pool in the dendrite by an element of $\langle \alpha, \beta, \delta \rangle$.*

The next lemma takes a somewhat different form, and leads directly into the main result of this chapter.

Lemma 3.2.5. *Let S be a finite arc diagram for the dendrite. Then there exists some element $g \in \langle \gamma, \beta^\dagger \rangle$ such that the image of S under g has the same number or fewer arcs as S, and has no arcs other than P, the central pool arc, that lie between A and A'.*

Proof. Let n be the number of arcs in S that lie between A and A'. We will proceed by induction on n.

Base case: Suppose $n = 0$ or $n = 1$. Then there are no arcs in S that lie between A and A' beside P.

Now suppose $n > 1$. Then at least one of the children of the central pool must be included in S. In the first case, suppose that P_L, the left child of the central pool, is included in S. Then we can see that under the action of γ, P_L is moved to A', and thus, P_L and any arcs that lie to the right of it in S, no longer lie between A and A' in $\gamma(S)$.

Thus, since the central pool must have been included in the original lamination, and lies to the right of P_L, $\gamma(S)$ contains at most $n-2$ arcs. Also note that because A, A', P, and P_L are the only arcs in the domain lamination for γ, this action does not require the inclusion of any arcs that were not already included in S, and thus, cannot increase n.

In the second case, suppose that P_R, the right child of the central pool, is included in S. Then we can see that under the action of $\beta^\dagger$, P_R is moved to A', and thus, P_R and any arcs that lie to the right of it in S, no longer lie between A and A' in $\beta^\dagger(S)$. Thus, $\beta^\dagger(S)$ contains at most $n-1$ arcs. Also note that because A, A', P, and P_R are the only arcs in the domain lamination for $\beta^\dagger$, this action does not require the inclusion of any arcs that were not already included in S, and thus, cannot increase n. □

We now present our main result for this section.

Theorem 3.2.6. *The elements $\langle \alpha, \beta, \delta \rangle$ generate the group T_D.*

Proof. Let $f \in T_D$. Then by Lemma 3.2.3, we may assume that f maps the main triple point, A, to itself. Furthermore, because A is fixed, we may compose f with α $0, 1$, or 2 times and ensure that each arm that branches from the triple point at A is mapped to itself.

Then let n be the number of objects in the reduced arc pair diagram for f. We will proceed by induction on n.

Base case: Suppose that $n = 2$. Then f is either the identity or δ, both of which are in $\langle \alpha, \beta, \delta \rangle$.

Now suppose $n > 2$. Then see that because A is fixed, if the reduced arc pair diagram for f contains more than one distinct child of A, we can write f as a composition of functions, each of which is the identity on all but one of the arms coming off of A, and each of which then has fewer than n objects in its reduced arc pair diagram. From that, we can see that each of these subfunctions is in $\langle \alpha, \beta, \delta \rangle$, and therefore, f is also in $\langle \alpha, \beta, \delta \rangle$.

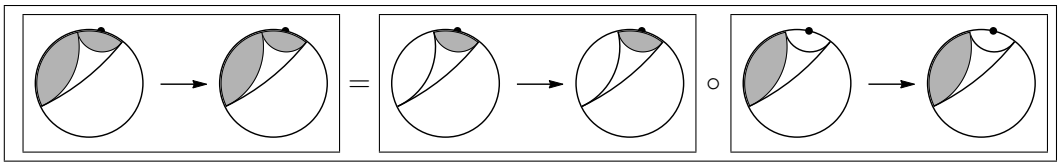

Figure 3.2.2: Splitting f into pieces when it has arcs under more than one arc of the main triangle.

Now suppose that the reduced arc pair diagram for f contains only one child of A. Then, by application of α, we may suppose that f is the identity on the arms $[1/7, 2/7]$ and $[2/7, 4/7]$, and has only got arcs between $4/7$ and $8/7$.

Now consider the arc pair diagram for f, and denote by f_D and f_R the domain and range laminations of f, respectively. By Lemma 3.2.5 there exist functions $\sigma, \tau \in \langle \gamma, \beta^\dagger \rangle$ such that $\sigma(f_D)$ and $\tau(f_R)$ each has no arcs other than the central pool between A and A', and such that the number of arcs in each does not increase. Also note that if either $\sigma(f_D)$ or $\tau(f_R)$ does contain the central pool arc, the other must as well, since that would imply that the object closest to A in the original lamination was a pool arc; because f must be an isomorphism of the lamination, that would have to be true of the other half of the diagram as well. Then we can write the composition $\tau \circ f \circ \sigma^{-1}$, and see that this new function has the same number or fewer arcs in its reduced arc diagram as f, and contains no arcs that lie between A and A', since if P is included, then it maps to itself, and may be removed.

Finally, we may conjugate this composition by δ, getting $\delta \circ \tau \circ f \circ \sigma^{-1} \circ \delta$. This new composition again fixes both A and A', but now the reduced arc pair diagram contains

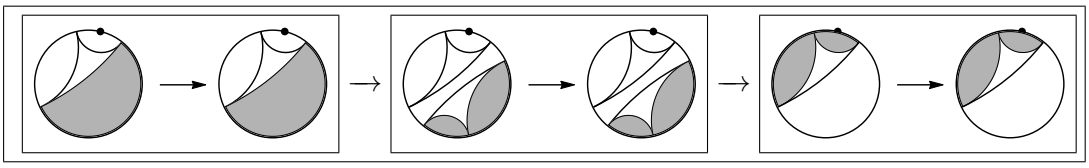

Figure 3.2.3: Reducing the number of arcs in the diagram for f.

no children of A', so we may remove the lower main triangle. Hence, the reduced arc pair diagram for $\delta \circ \tau \circ f \circ \sigma^{-1} \circ \delta$ contains at most $n-1$ objects, and is thus in $\langle \alpha, \beta, \delta \rangle$. Therefore, f is also in $\langle \alpha, \beta, \delta \rangle$. □

3.3 The Abelianization of T_D

In [1], Belk and Forrest showed that the commutator subgroup of T_B is simple by examining a two-coloring of the interior regions of the Basilica. In order to discover results about the commutator subgroup of T_D, we attempted to find a suitable coloring of the dendrite for which an analogous result could be proven, but in that were unsuccessful. We then turned to examining T_D^{ab}, the abelianization of T_D, as a means to gain insight about the commutator subgroup.

Because α has order 3, δ has order 2, and β has infinite order, the abelianization of T_D must be a quotient of $\mathbb{Z} \times \mathbb{Z}/2 \times \mathbb{Z}/3$, since every element of T_D can be written as a composition of α, β, and δ, so mapping an element to its abelianized form will simply count the number of α's (mod 3), the number of δ's, (mod 2), and the number of β's. However, it is not presently known whether the number of α's or δ's in an element is uniquely determined. We do, however, know that the number of β's in an element of T_D is uniquely determined.

Proposition 3.3.1. *There exists a homomorphism $\pi : T_D \longrightarrow \mathbb{Z}$ so that $\pi(\beta) = 1$.*

Proof. Let P be a pool in the dendrite, and let $f \in T_D$. Then, letting $\mathcal{P}$ be the set of pools in the dendrite, we define a function $h : \mathcal{P} \times T_D \longrightarrow \mathbb{Z}$, determined as follows. Let a, b, c, d be the slopes of f on the four intervals on which f is linear that have one endpoint at P, labelled counterclockwise so that the union of the intervals with slopes a and b is connected, as is the union of the intervals with slopes c and d, as shown in Figure 3.3.1.

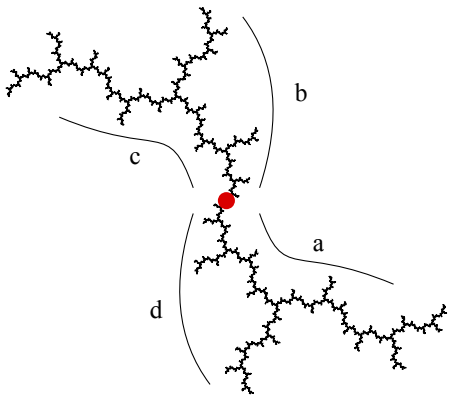

Figure 3.3.1: The labelling of slopes around the central pool.

Then we define

$$h(P, f) = \log_2(\frac{ac}{bc}).$$

Now we define $\pi : T_D \longrightarrow \mathbb{Z}$ by the rule

$$\pi(f) = \sum_{P \in \mathcal{P}} h(P, f).$$

To see that this is well-defined is trivial, since the slopes of f around any point are uniquely determined. Additionally, since $a = b = c = d$ for all but finitely many points for all $f \in T_D$, π will always be finite.

Now we will show that π is a homomorphism. Let $f, g \in T_D$, and let $P \in \mathcal{P}$. We see that

$$h(P, f \circ g) = h(P, g) + f(g(P), f)$$

since the slopes of $f \circ g$ around P are the product of the slopes of g around P and the slopes of f around the image, $g(P)$, so we can separate the logarithm as a sum. Then we see that

$$\pi(f \circ g) = \sum_{P \in \mathcal{P}} h(P, g) + \sum_{P \in \mathcal{P}} h(g(P), f)$$

but since $g \in T_D$, it preserves the set of pools in the dendrite, so we see that this is equivalent to

$$\pi(f \circ g) = \sum_{P \in \mathcal{P}} h(P, g) + \sum_{P \in \mathcal{P}} h(P, f) = \pi(g) + \pi(f).$$

Therefore, π is a homomorphism.

To prove that $\pi(\beta) = 1$, observe that β has only one breakpoint located at a pool, which is at the central pool, so for all pools other than the central pool, $a = b = c = d$, and $h(P, \beta) = 0$. For P the central pool, $h(P, \beta) = \log_2(\frac{8 \cdot 1}{4 \cdot 1}) = \log_2(2) = 1$. Thus, $\pi(\beta) = 1$. □

Having shown this, the next result follows as an immediate corollary.

Corollary 3.3.2. *The abelianization of T_D is an infinite quotient of $\mathbb{Z} \times \mathbb{Z}/3 \times \mathbb{Z}/2$; equivalently, $[T_D, T_D]$ has infinite index.*

Proof. By the previous proposition, we know that the abelianization contains a copy of $\mathbb{Z}$. Additionally, we know that $\langle \alpha \rangle \cong \mathbb{Z}/3$ and $\langle \delta \rangle \cong \mathbb{Z}/2$, so if there were no relations in T_D other than $\alpha^3 = \delta^2 = 1$, the abelianization would be isomorphic to $\mathbb{Z} \times \mathbb{Z}/3 \times \mathbb{Z}/2$; hence, we know that it must be a quotient of that. In particular, we see that T_D^{ab} must be isomorphic to one of the following: $\mathbb{Z}$, $\mathbb{Z} \times \mathbb{Z}/2$, $\mathbb{Z} \times \mathbb{Z}/3$, or $\mathbb{Z} \times \mathbb{Z}/3 \times \mathbb{Z}/2$. □

We are also able to show that the abelianization is virtually cyclic.

Definition 3.3.3. A group is **virtually cyclic** if it contains a cyclic subgroup of finite index.

Corollary 3.3.4. *The abelianization of T_D is virtually cyclic.*

Proof. Because we have classified the possible isomorphism types of T_D^{ab}, and all of them are virtually cyclic, T_D^{ab} must be virtually cyclic. □

Though Schrier's lemma states that if the abelianization is finite, and the commutator subgroup has finite index, that the commutator subgroup is then finitely generated, the converse is not, in general true. Nonetheless, we present the following as a conjecture.

Conjecture 3.3.5. *The commutator subgroup $[T_D, T_D]$ is not finitely generated.*

We also present the full result about the structure of the abelianization of T_D as a conjecture.

Conjecture 3.3.6. *The abelianization of T_D is isomorphic to $\mathbb{Z} \times \mathbb{Z}/2 \times \mathbb{Z}/3$.*

3.4 Diagram Groups

While Belk and Forrest's Basilica group is one generalization of Thompson's groups, there exist many others beside. In particular, one that is of interest is a family of groups presented by Guba and Sapir in [5] called Diagram Groups. Diagram groups are of interest here because, much in the way that there exist copies of T lying inside of T_B, there exist copies of a two diagram groups, which we will refer to as the segment group and the pool group, lying inside of T_D, and this is of use to us in understanding its structure.

Diagram groups are formed by creating labelled partitions of the unit interval in a manner similar to that used in F, and then defining piecewise-linear functions between them.

Definition 3.4.1. A **labelled partition** of the unit interval is a partition of the unit interval and a sequence of symbols that correspond to each piece of the partition.

Definition 3.4.2. An **alphabet** is a set, whose elements are called **symbols**.

Definition 3.4.3. A **word** is a finite sequence of symbols.

Definition 3.4.4. A **replacement rule** is a pair of the form $A \longrightarrow \omega$ where A is a symbol, and ω is a word.

Definition 3.4.5. Let T be a labelled partition. Then an **expansion** of T is a labelled partition that is identical to T on all but one piece of the partition, where if A is the label for that segment of the partition, and $A \longrightarrow \omega$ is a replacement rule and ω has length n, that segment has been partitioned into n pieces, which are labelled by ω.

Definition 3.4.6. A **labelled piecewise-linear function** from the unit interval to itself is a piecewise-linear function from the unit interval to itself where both the domain and range are labelled partitions that have the same sequence of symbols corresponding to their pieces.

For example, begin with the unit interval.

Partition it in some finite number of pieces, which need not be dyadic.

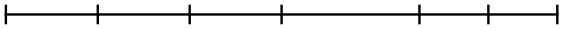

Label the pieces with some collection of symbols.

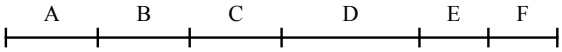

The result is a labelled partition. Now let $D \longrightarrow BBAD$ be a replacement rule. Then we can create an expansion of the above labelled partition thus.

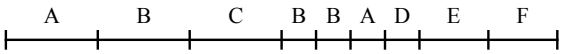

To form a labelled piecewise-linear function, we simply choose two labelled partitions that have the same sequence of symbols for labels, and map linearly between them.

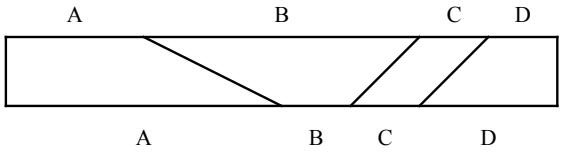

We are now able to define a diagram group.

Definition 3.4.7. A diagram group $D(\Sigma, \mathcal{R}, \omega)$ is a group determined by an alphabet, Σ, a set of replacement rules, $\mathcal{R}$, and a starting word, ω consisting of symbols in Σ. The group consists of labelled piecewise-linear functions from the unit interval to itself whose domain and range are both labelled partitions that can be created by expanding the starting word a finite number of times according to the replacement rules in $\mathcal{R}$.

We will now show that Thompson's group F can be understood as a diagram group.

Example 3.4.8. Recall that Thompson's group F is formed from dyadic rearrangements of the unit interval. In particular, the function X_0 is the one defined as follows:

$$f(x) = \begin{cases} 2x & \text{if } 0 \leq x \leq 1/4 \\ x + 1/4 & \text{if } 1/4 \leq x \leq 1/2 \\ 1/2x + 3/4 & \text{if } 1/2 \leq x \leq 1. \end{cases}$$

We can define a diagram group that is identical to F as follows. Let our alphabet be the set $\{A\}$, let our starting word be A, and let our replacement rule be $A \longrightarrow AA$. In this way, if we begin with the unit interval, labelled A

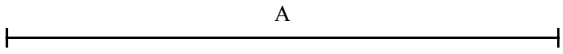

and then perform the expansion $A \longrightarrow AA$ a finite number of times, we have a dyadic subdivision of the unit interval.

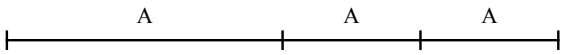

Then if we choose another labelled partition with the same sequence (i.e., three A's), and map linearly from the first to the second, we form a labelled piecewise-linear function, which is an element of F.

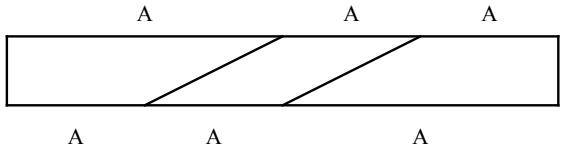

It quickly becomes clear that any element of F may be represented in this way; hence, F can be seen to be a diagram group.

There is another way to represent elements of a diagram group, without drawing the rectangle diagram, which we will make use of in the next two sections. In this way, expansions are denoted by putting the expanded symbols in parentheses. For example, if ABC is a word in our diagram group, and $B \to DE$ is a replacement rule, then we may write an expansion of ABC as $A(DE)C$. Then alternate parenthesizations of the same sequence of symbols correspond to different labelled partitions of the interval that have the same sequence of symbols, and we may thus write labelled piecewise-linear functions as reparenthesizations of a sequence of symbols.

For example, the function we made a rectangle diagram for in Example 3.4.8 was X_0, which is a generator for F. Using the same alphabet, we can write X_0 simply as

$$A(AA) \to (AA)A.$$

For a slightly more complicated example, if we have the alphabet $\{A, B\}$ and the replacement rules$A \to AB$ and $B \to BA$, and starting word AB, then we begin with the following diagram.

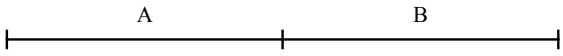

If we apply the $A \to AB$ replacement rule to the first piece, and then apply the $B \to BA$ replacement rule to the second piece of that, we arrive at this partition.

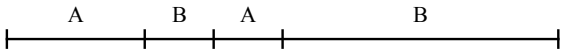

If we instead apply the $B \to BA$ rule first, and then apply the $A \to AB$ rule to the resultant A, we arrive at this partition.

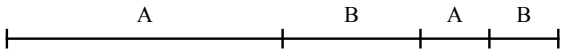

Since these two partitions both have the same sequence of symbols, we may create a labelled piecewise-linear map between them, as follows.

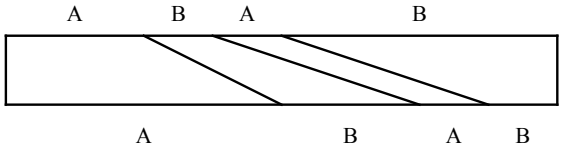

If we wish to represent this as a reparenthesization, however, we see that the domain is achieved by the replacements $AB \to (AB)B \to (A(BA))B$, and the range is achieved by the replacements $AB \to A(BA) \to A(B(AB))$. Thus, we can represent this function by reparenthesization as

$$(A(BA))B \to A(B(AB)).$$

The diagram groups that we have defined are actually a special case of the diagram groups defined by Guba and Sapir in [5]; their diagram groups allow for replacement rules that map words to words, rather than just symbols to words, but allowing that makes it much more difficult to visually represent elements of the groups. Because this version of diagram groups is sufficient for the present work, we will not use the more general form.

3.5 Generators and Presentations for Diagram Groups

Guba and Sapir present a number of strong results for diagram groups that allow insight into their structure. In particular, they allow us to discover results about the generating sets and presentations for diagram groups. To state these theorems, we must first give some definitions.

Definition 3.5.1. Let $D(\Sigma, \mathcal{R}, \omega)$ be a diagram group. Then an **allowable word** in D is a word that can be created by performing expansions of ω.

Definition 3.5.2. Let $D(\Sigma, \mathcal{R})$ be a diagram group, and let P be an allowable word in D. Then a **reduction** of P is the inverse of an expansion. Two reductions are said to **overlap** if the intersection of the letters they act on is nonempty.

Definition 3.5.3. Let $D(\Sigma, \mathcal{R})$ be a diagram group, and let P be an allowable word in D. Then the **reduction graph** for P is a graph with one vertex for each reduction of P, and an edge between each pair of vertices corresponding to reductions that do not overlap.

Definition 3.5.4. Let $D(\Sigma, \mathcal{R})$ be a diagram group, and let P be an allowable word in D. The **reduction complex** is the simplicial complex obtained by pasting in a triangle along each cycle of length three in the reduction graph.

We now have two important results that will be made use of in the next section, both of which are proved in [5].

Theorem 3.5.5. *Let D be a diagram group. If the reduction graph is connected for all but finitely many allowable words T, then D is finitely generated.*

Theorem 3.5.6. *Let D be a diagram group. If the reduction complex is connected and simply connected for all but finitely many allowable words T, then D is finitely presented.*

3.6 Diagram Groups Contained in T_D

We can construct several diagram groups as subgroups of T_D. In particular, we are interested in diagram groups that represent by letter substitutions the way that the self-similar structure of the dendrite reveals multiple copies of the same structure at various scales. For example, the first such group we will examine attempts to describe some of the structure that is found in a segment of the dendrite, between two triple points.

As we know, every segment contains three smaller segments, separated from each other by an up arm and a down arm, as seen in Figure 3.6.1. To represent this, we choose the alphabet $\Sigma = \{S, U, D\}$ the replacement rule $S = SUSDS$, and the starting word

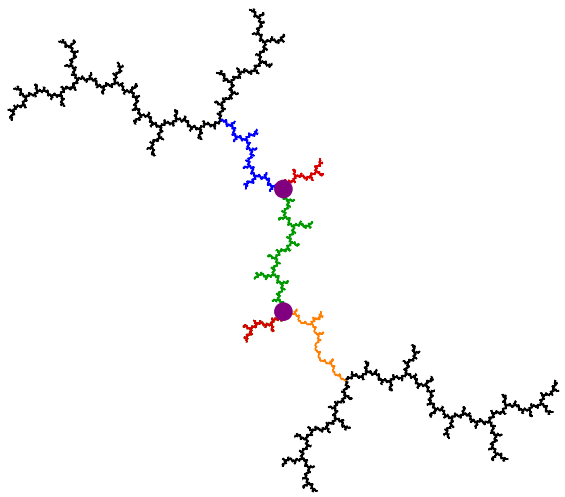

Figure 3.6.1: Each segment contains three smaller segments.

S. We call this the **segment group**. Unfortunately, it is difficult to say much about its structure, since our primary tool, Theorem 3.5.5 is not useful when there are infinitely many allowable words that have disconnected reduction graphs. One might expect that that would be enough to state that the group is not finitely generated, but it is not; all we know is that one method for proving that the segment group is finitely generated does not work.

Proposition 3.6.1. *The segment group has infinitely many words with disconnected reduction graphs.*

Proof. Observe that $SUSDSUSDS$ is an allowable word in the segment group, since it can be obtained by

$$S \to SUSDS \to (SUSDS)USDS.$$

Then observe that $SUSDSUSDS$ has two reductions, namely

$$(SUSDS)USDS \to SUSDS$$

$$SUSD(SUSDS) \to SUSDS.$$

Because these two reductions overlap, the reduction graph for $SUSDSUSDS$ is simply two disconnected vertices. Then by Theorem 3.5.5, the element $(SUSDS)USDS \to SUSD(SUSDS)$ is a generator of the segment group.

Now observe that this same argument holds for $SU(SUSDSUSDS)DS$, as well as for $SU(SU(SUSDSUSDS)DS)DS$, and in fact, for any word beginning with some finite number of copies of SU, followed by $SUSDSUSDS$, followed by the same number of copies of DS at the end. Hence, there are infinitely many words in the segment group with disconnected reduction graphs. □

This result is somewhat disappointing, because if the segment group had been finitely generated, we might have hoped it would be finitely presented as well, which might have allowed us to find some relations in the dendrite group. However, no such result presented itself.

We now turn instead to a different diagram group, which models the structure of the dendrite between two pools. In this particular construction, however, we allow points like the endpoint $z = i$ to count as pools, since $z = i$ is the image of the central pool under ϕ. Observe, then, that we can partition the geodesic from the central pool to i into the left half of a segment, from the central pool to the 11/112 arm, an entire segment, from that arm to the main triple point, and the right half of a segment, from the main triple point to $z = i$. Each of these half-segments can, in turn, be partitioned into an entire segment and another half segment, as seen in 3.6.2.

Because of this partitioning, we choose to construct this diagram group as follows. We choose the alphabet $\Sigma = \{L, R, U, D\}$, the replacement rules $L \to LDRL$ and R

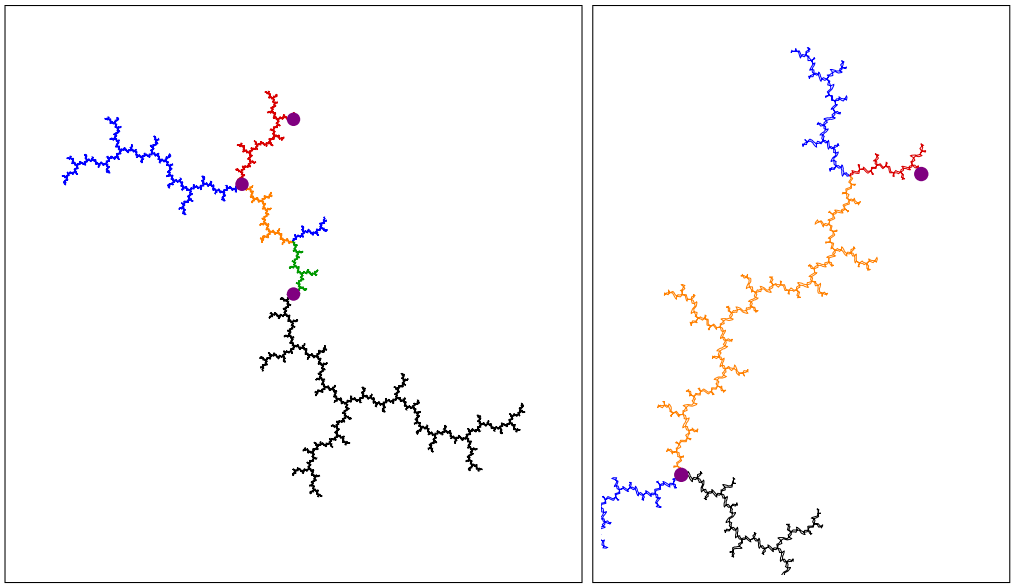

Figure 3.6.2: First: Partitioning the section of the dendrite between the central pool and $z = i$. Second: Further partitioning the half-segment between the main triple point and $z = i$.

$\rightarrow RLUR$ and the starting word $LDRLUR$. It will be seen that this group has much nicer properties than the previous group, in spite of being in some ways very similar to it. We will call this the pool group.

Proposition 3.6.2. *The pool group is finitely generated.*

Proof. We will again use Theorem 3.5.5 to prove this result. First observe that on any allowable word in this, any two reductions can only overlap if they are adjacent. From this, we can deduce that no word with four or more reductions can have a disconnected reduction graph, since the first vertex must share an edge with every vertex other than the second, and the second vertex must share an edge with every vertex other than the fist and third, so both the first and second vertices are connected to the fourth, making the graph connected. Hence, it will suffice to show that there can only be finitely many allowable words with three or fewer reductions.

We will show this by demonstrating that every time the length of a word is increased, the number of allowable reductions is increased. Let T be an allowable word in the pool group, and suppose that a substitution that increases the length of T is made. Then we know that the substitution was either $L \to LDRL$ or $R \to RLUR$. In the first case, if the L occupied either the first or last L of another $LDRL$ string, then that string is preserved, since we have either $LDR(LDRL)$ or $(LDRL)DRL$. If the L occupied the second L of an $RLUR$ string, then that string is also preserved, since we have $R(LDRL)UR$. Thus, if the substitution was $L \to LDRL$, no reduction that was previously allowed is now unavailable. The same argument holds for the substitution $R \to RLUR$. Hence, in either case, every reduction that could be made in T can be made in the expanded word. Since the expansion can also be undone as a reduction, the expanded word has one more reduction than T. Thus, only finitely many words in the pool group can have disconnected reduction graphs, so the pool group is finitely generated. □

It is of interest to note that a generating set for the pool group is formed by the elements

$$(LDRL)DRLUR \to LDR(LDRL)UR$$

$$LD(RLUR)LUR \to LDRLU(RLUR)$$

$$(LDRL)DRLDRLUR \to LDR(LDRL)DRLUR$$

$$LD(RLUR)LURLUR \to LDRLU(RLUR)LUR,$$

but as we have seen, this is not essential to the proof of Proposition 3.6.2. This fact would be of particular interest had we not already developed a generating set for T_D, but at present, it is simply a curiosity. In our search for relations on T_D, we have also got the following proposition.

Proposition 3.6.3. *The pool group is finitely presented.*

Proof. Let T be an allowable word in the pool group, and suppose T has at least 9 reductions. We will show by induction that the reduction graph for T is simply connected. Note first that every loop in the reduction complex is homotopic to a closed path of edges in the reduction graph. Let L be such a closed path of edges in the reduction graph for T, and suppose L has n vertices. We must show that L is nullhomotopic.

Base case: Suppose $n = 4$. Then every vertex of L can have at most two other vertices in the reduction graph that it is disconnected from. Hence, there are at most 8 vertices of the reduction graph that are not connected to every vertex of L. But T has at least 9 reductions, so there exists some vertex of the reduction graph that is connected to every vertex of L. Therefore, L can be contracted to a single point, and is thus nullhomotopic.

Inductive case: Suppose $n > 4$. Then let a_1, a_2, a_3, a_4 be sequential vertices in L. Then by the argument from the previous case there exists some other vertex v such that v shares an edge with each of a_1, a_2, a_3, a_4. Then the path $a_1 \longrightarrow a_2 \longrightarrow a_3 \longrightarrow a_4$ is homotopic to the path $a_1 \longrightarrow v \longrightarrow a_4$, thus reducing the number of vertices of L by one. By our inductive hypothesis, then, the number of vertices of L can be reduced to one, and thus, every loop in the reduction complex is nullhomotopic.

By the argument from the proof of Proposition 3.6.2, then, we can see that there must be only finitely many allowable words in the pool group that have a reduction graph that is not simply connected. Thus, by Theorem 3.5.6, the pool group is indeed finitely presented. □

Unfortunately, the fact that we must require a word with at least 9 reductions in order to prove that the reduction graph is simply connected means that it is very difficult to compile a list of all such words and in attempting to do so, we found that, of the ones we checked, the relations that they produced were trivial in T_D, so we stopped pursuing that avenue.

3.7 Other Groups Contained in T_D

It is known that the modular group, Γ acts on the infinite tree with alternating two-edge and three-edge vertices by rotation around around the central two-edge vertex and rotation around the central three-edge vertex. We will make use of this fact to prove that there is a subgroup of T_D isomorphic to Γ.

Theorem 3.7.1. *The group $\langle \alpha, \delta \rangle$ is isomorphic to Γ.*

Proof. We will prove this result by finding a copy of the tree that Γ acts on within the dendrite. Let the first vertex be the main triple point. Because we know that each arm of the main triple point is a branch arm, we know that each arm is partitioned into two branch arms and a segment. Add one vertex for the pool located at the center of each of these segments, and an edge connecting each of these vertices to the main triple point. Then add a vertex for the dominant triple point on each arm, and an edge connecting each to its corresponding pool. Then for each such triple point, repeat the process on each branch arm, continuing infinitely. In this way we construct an infinite tree with alternating two-edge and three-edge vertices that lies within the dendrite. Because α represents a one-third rotation around the main triple point, and δ represents a one-half rotation around the central pool, we see that the set $\{\alpha, \delta\}$ acts on this tree in the same manner as the generators of Γ do. Therefore, $\langle \alpha, \delta \rangle \cong \Gamma$. □

Corollary 3.7.2. *The group $\langle \alpha, \delta \rangle$ is isomorphic to $\mathbb{Z}/3 * \mathbb{Z}/2$, and as such, has no relations other than $\alpha^3 = \delta^2 = i$.*

Proof. It is shown in [8] that $\Gamma \cong \mathbb{Z}/3 * \mathbb{Z}/2$, so the result is immediate. □

Theorem 3.7.3. *There is a subgroup of T_D that is isomorphic to Thompson's Group F.*

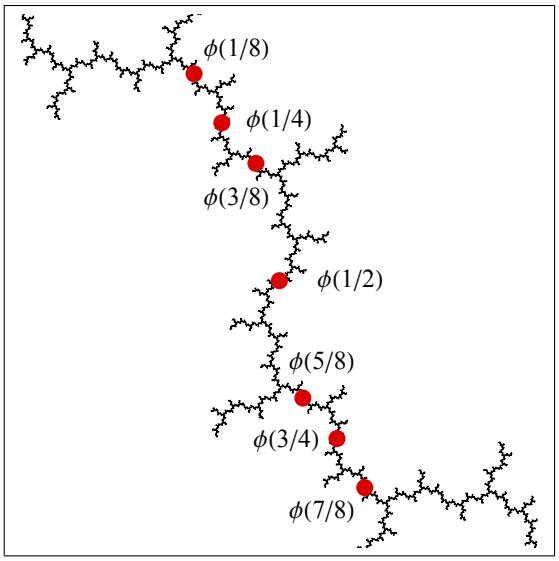

Figure 3.7.1: Some of the dyadic points on the dendrite.

Proof. Let ϕ be a map from the dyadic points in $[0,1]$ to the pool arcs in the central segment of the dendrite that is defined in the following way. Let $\phi(1/2)$ be the central pool arc. Since the central segment has a basic partition, let $\phi(1/4)$ be the pool arc that dominates the left segment of the basic partition, and let $\phi(3/4)$ be the pool arc that dominates the right segment. We continue making dyadic subdivisions by mapping the midpoints of the two intervals adjacent to any dyadic point to the pool arcs that dominate the left and right segments of the basic partition of the segment that that dyadic point's pool arc dominates. In this way, we see that ϕ is an injective map from the dyadic points of the unit interval to the pool arcs of the dendrite. Thus, to show that there is a subgroup of T_D isomorphic to F, we must simply show that there are elements of T_D that act on the images of the dyadic points in the way that X_0 and X_1 do.

For X_0, we need to find an element of T_D that maps $\phi(1/2)$ to $\phi(1/4)$, maps $\phi(3/4)$ to $\phi(1/2)$, and preserves the set of the images of the dyadic points. We know that $\phi(1/2)$ is the central pool, P, $\phi(1/4)$ is the pool that dominates the left-side segment, which we denote P_L and has arcs $\{13/96, 55/96\}$, and $\phi(3/4)$ is the pool that dominates the right-

side segment, which we denote P_R, and has arcs $[7/96, 61/96]$. Thus, our function will map P_R to P, and P to P_L, and act linearly on the sections of the dendrite that lie between them. It turns out that we can write this as a piecewise-linear function on the external angles

$$\phi \circ X_0(\theta) = \begin{cases} \theta & \text{if } 0 \leq \theta \leq 1/14 \\ 8\theta - 1/2 & \text{if } 1/14 \leq \theta \leq 71/896 \\ \theta + 7/128 & \text{if } 71/896 \leq \theta \leq 9/112 \\ \theta/8 + 1/8 & \text{if } 9/112 \leq \theta \leq 1/7 \\ \theta & \text{if } 1/7 \leq \theta \leq 4/7 \\ \theta/8 + 1/2 & \text{if } 4/7 \leq \theta \leq 71/112 \\ \theta - 7/128 & \text{if } 71/112 \leq \theta \leq 569/896 \\ 8\theta + 1/2 & \text{if } 569/896 \leq \theta \leq 9/14 \\ \theta & \text{if } 9/12 \leq \theta \leq 1 \end{cases}$$

To construct an arc pair diagram for this function, we also need to include the parent of $\phi(3/4)$, which is the triple point $\{9/112, 67/112, 71/112\}$, and its image, $\{121/896, 515/896, 519/896\}$, as well as the parent of $\phi(1/4)$, which is the triple point $\{11/112, 15/112, 65/112\}$, and its preimage, $\{67/896, 71/896, 569/896\}$. Having done so, we have successfully created an arc pair diagram for $\phi \circ X_0$; therefore, $\phi \circ X_0 \in T_D$. To show that $\phi \circ X_0$ preserves the set of dyadic points, simply observe that all of the slopes are either 1/8, 1, or 8, and the offsets are all powers of two, so anything with a denominator equal to $12 \cdot 2^n$, and numerator equal to 7 plus a power of two, will be mapped to something else with those same conditions; thus, the pools in the central segment are preserved.

For X_1, we need an element of T_D that maps $\phi(7/8)$ to $\phi(3/4)$, and maps $\phi(3/4)$ to $\phi(5/8)$ and preserves the set of the images of the dyadic points. We recall that $\phi(3/4)$ is P_R. We see that $\phi(5/8)$ is the pool that dominates the left-side segment of P_R, and has arcs $\{61/768, 487/768\}$, and $\phi(7/8)$ is the pool that dominates the right-side segment of P_R, and has arcs $\{55/768, 493/768\}$. Thus, we construct a piecewise function that exerts

the desired mapping on the dendrite, given by

$$\phi \circ X_1(\theta) = \begin{cases} \theta & \text{if } 0 \leq \theta \leq 1/14 \\ 8\theta + 1/2 & \text{if } 1/14 \leq \theta \leq 519/7168 \\ \theta + 7/1024 & \text{if } 519/7168 \leq \theta \leq 65/896 \\ \theta/8 + 9/128 & \text{if } 65/896 \leq \theta \leq 9/112 \\ \theta & \text{if } 9/112 \leq \theta \leq 71/112 \\ \theta/8 + 71/128 & \text{if } 71/112 \leq \theta \leq 575/896 \\ \theta - 7/1024 & \text{if } 575/896 \leq \theta \leq 4601/7168 \\ 8\theta + 1/2 & \text{if } 4601/7168 \leq \theta \leq 9/14 \\ \theta & \text{if } 9/14 \leq \theta \leq 1 \end{cases}$$

To construct an arc pair diagram, we also need to include the parent of $\phi(3/4)$, which is the triple point $\{9/112, 67/112, 71/112\}$, as well as the central pool, the lower triple point, and the main triple point. Additionally, to the domain piece of the diagram, we add the parent of $\phi(7/8)$, which is the triple point with angles $\{65/896, 571/896, 575/896\}$ and the preimage of the parent of $\phi(5/8)$, which is the triple point with angles $\{515/7169, 519/7168, 4601/7168\}$. To the range piece of the diagram, we add the parent of $\phi(5/8)$, which is the triple point with angles $\{67/896, 71/896, 569/896\}$, and the image of the parent of $\phi(7/8)$, which is the triple point with angles $\{569/7168, 4547/7168, 4551/7168\}$. Having done so, we have successfully created an arc pair diagram for $\phi \circ X_1$; therefore $\phi \circ X_1 \in T_D$. To show that $\phi \circ X_1$ preserves the set of dyadic points, simply observe that all of the slopes are either 1/8, 1, or 8, and the offsets are all powers of two, so anything with a denominator equal to $12 \cdot 2^n$, and numerator equal to 7 plus a power of two, will be mapped to something else with those same conditions; thus, the pools in the central segment are preserved.

Having constructed these functions, we can see that $\langle \phi \circ X_0, \phi \circ X_1 \rangle$ must indeed be isomorphic to F, and the result is proven. □

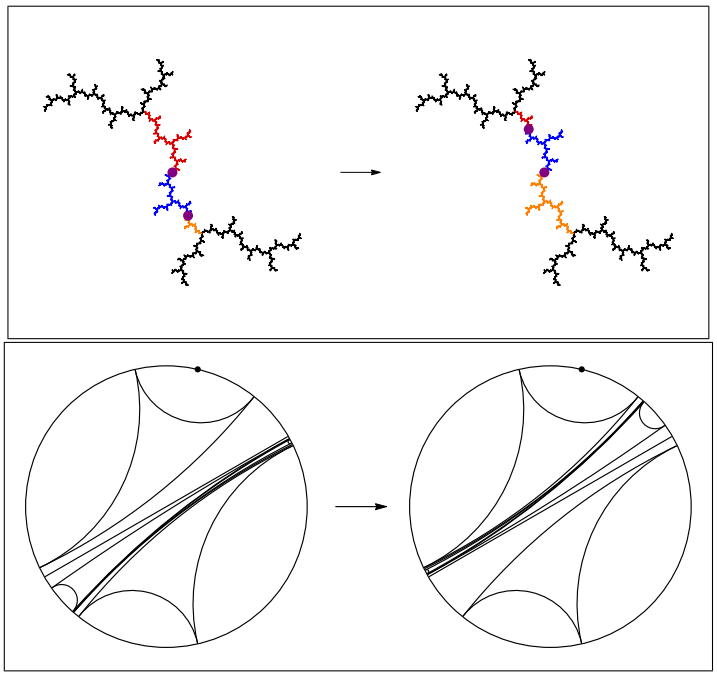

Figure 3.7.2: Top: The action of $\phi \circ X_0$ on the dendrite. Bottom: The arc pair diagram for $\phi \circ X_0$.

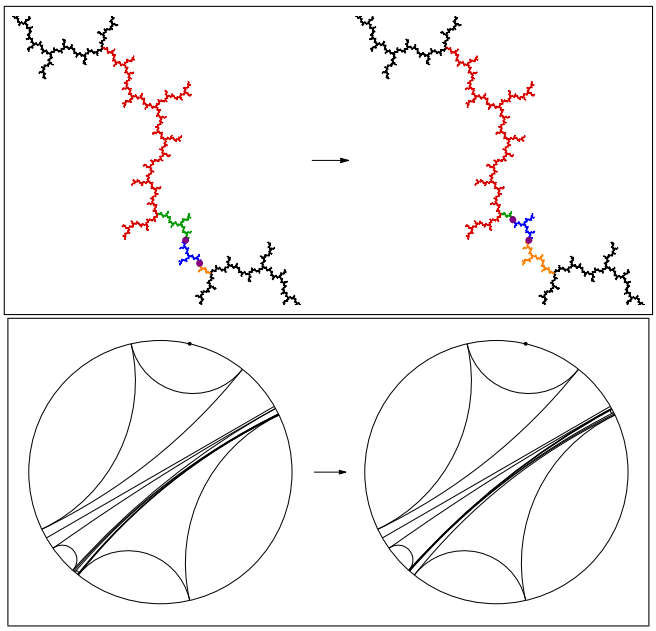

Figure 3.7.3: Top: The action of $\phi \circ X_1$ on the dendrite. Bottom: The arc pair diagram for $\phi \circ X_1$.

4
The Group T_D^* on Arbitrary Dendrites

4.1 Arbitrary Dendrites

There are many other dendrites that can be found by the method of choosing an iterate of zero to be periodic, and choosing a period length for that point. Many of these other dendrites bear some resemblance to the $c = i$ dendrite, and in this chapter, we will try to give some characterization of that resemblance, and make conjectures about ways in which T_D might be generalized to apply to them.

In Figure 4.1.1, we see six other dendrites, with red dots marking the orbits of zero in each. The first image is the dendrite for $c = -0.228155 + 1.11514i$, and is found by choosing the third iterate of zero to be fixed. The second, third and fourth images are the dendrites for $c = -1.23923 + 0.412602i$, $c = -0.155788 + 1.11222i$, and $c = 0.395014 + 0.555625i$, respectively, and are all found by choosing the second iterate of zero to have period 3. The fifth and sixth images are the dendrites for $c = -0.101096 + 0.956287i$, and $c = 0.343907 + 0.70062i$, respectively, and are found by choosing the fourth iterate of zero to be fixed.

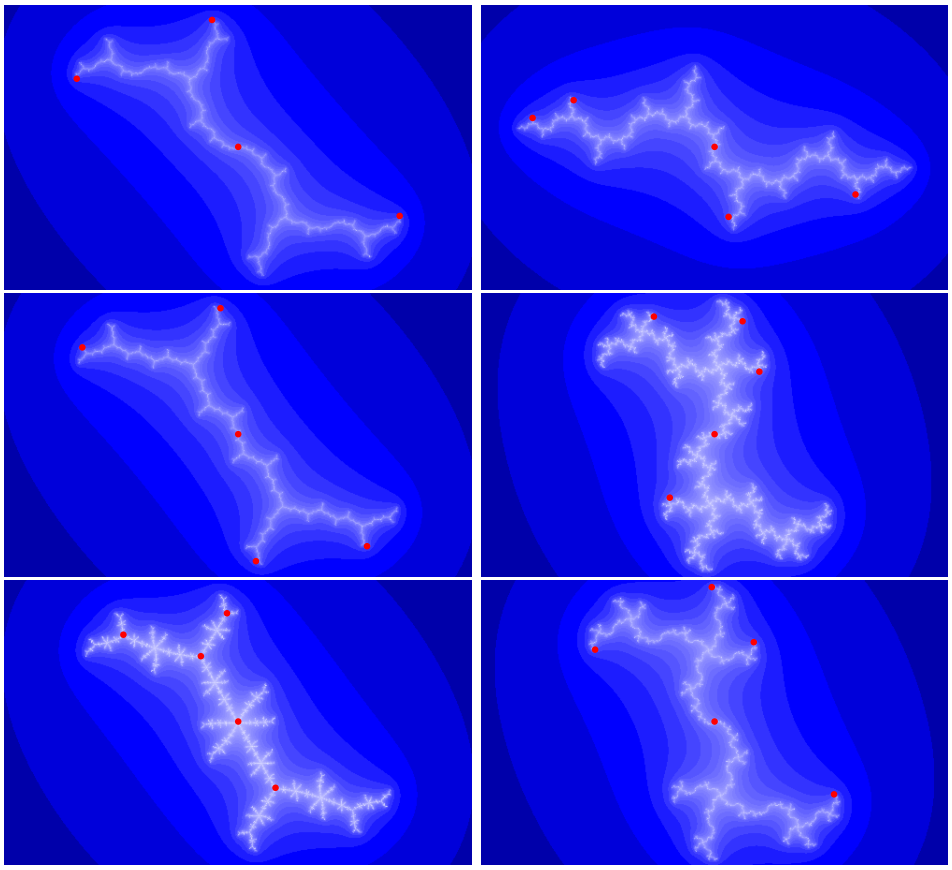

Figure 4.1.1: Some other dendrites with the orbits of zero marked.

In general, it seems that most of these dendrites share the property with the $c = i$ dendrite that they have two main kinds of points: pools, and some kind of branching point at the fixed point. One interesting thing to note is that, in the fifth image, the orbit of zero includes several of those branching points, including the fixed point. This suggests that, where the denominators of external rays for the central pool and the triple point in the $c = i$ dendrite were relatively prime, that this is not necessarily always the case; indeed, there must be some number of doublings that will map the angles for the central pool in that dendrite to the angles for the fixed point.

We also observe that, in general, most structural properties of the $c = i$ dendrite are preserved. Though there may be different numbers of branchings, there is always a branch

point located between the fixed point and the central pool, and it seems reasonable to suppose that this branch point in general is mapped to the point corresponding to the dominant triple point of the upward-facing arm of the fixed point. Additionally, it seems to be the case that on a branch arm, the dominant point of that branch arm always partitions the branch arm into two branch arms and a segment, and that in a segment, the preimages of the points corresponding to $\{11/112, 15/112, 65/112\}$ and $\{9/112, 67/112, 71/112\}$ partition the segment into three smaller segments. Though it is true that in some of the dendrites the arm or arms branching off of those points is facing in the opposite direction from its corresponding arm in the $c = i$ dendrite, this probably does not have much effect on the overall structure.

One particularly striking difference from the $c = i$ dendrite is that the dendrite shown in the fifth picture branches in six directions at the central pool, and it seems to be the case that only the dominant points of branch arms branch in three directions. Because of this, it seems that the point corresponding to the left-side child of the central pool cannot be mapped to the fixed point, as we would do with β, since they have different numbers of arms. From this fact it seems clear that an analogous group acting on this dendrite cannot be the same as T_D. On the other dendrites, however, it seems very likely that a group very similar, or even isomorphic to T_D might be found. In particular, in the first, second, and third images, since the fixed points of those dendrites branch in three directions, and there are no branchings at the pools, we can conjecture that a group isomorphic to T_D might be found. On the dendrites in the fourth and sixth images, it seems likely that a group in which α had order 4 instead of order 3 might act exactly as desired.

4.2 The Group T_D^*

In this section, we outline a path to constructing groups acting on other dendrites. We will refer to a dendrite that branches in n directions at the fixed point and in m directions

at the central pool as an **(n, m)-dendrite**. We will particularly focus on $(n, 2)$-dendrites, since they are the ones most analogous to the $c = i$ dendrite, but some of the things we discuss will carry over in generality.

The first thing that needs to be gotten working is the notion of segments and branch arms. It seems likely that this will just carry over exactly from the notions presented for $c = i$; certainly analogous structures seem to exist in the other dendrites. When this is constructed, it can be used to define ancestry; again, this seems as though it will carry over exactly as desired to generality; if a branch arm is partitioned into a segment and four branch arms, then the dominant pool of that segment and the dominant points of each of the small branch arms are the children of the dominant point for the original branch arm. In general, a point R is an ancestor of S if, as before, S lies in a branch arm having R as the base point, or S lies in a segment having R as an endpoint, or S lies in a segment having R as the dominant pool. Since none of these things are dependent on the number of branchings at any given point, it seems plausible that ancestry will work without any modification needed.

From ancestry, one can develop arc pair diagrams, and finite tree diagrams to represent dyadic rearrangements of these new dendrites; presumably the constructions will be more or less analogous. Also note that because these dendrites arise from postcritically finite polynomials, it will always be the case that all of the external rays land as desired, as we discussed in chapter 2. Because we expect all of these constructions to be possible, we predict that the set of all dyadic rearrangements of an arbitrary dendrite, which we will denote $\boldsymbol{T_D^*}$, will form a group under composition.

For T_D^*, when D is an $(n, 2)$ dendrite, we conjecture that a generating set can be found as follows. The first generator, α^* will be a rotation around the fixed point such that each arm of the fixed point is mapped to the next counterclockwise arm. The second generator, δ^* will be a rotation around the central pool so that the fixed point is mapped to the point

corresponding to the lower triple point, and vice versa. The third generator, β^* will be a function that is fixed below the central pool, and maps the left-side child of the central pool to the fixed point. Note that the existence of β^* is why we require that D be an $(n, 2)$ dendrite, since in our example of a dendrite with more branchings at the central pool, such a function does not seem to be possible.

Observe that in the $c = i$ dendrite, the generators $\alpha^*, \beta^*, \delta^*$ correspond exactly to the generators α, β, δ. Thus, for any other $(3, 2)$ dendrite, it should be possible to define a isomorphism $T_D^* \to T_D$ by simply mapping α^* to α, β^* to β, and δ^* to δ. For $(n, 2)$ dendrites when n is at least four, the group will probably be similar; it seems reasonable to expect that the abelianization will again be infinite and virtually cyclic, and probably isomorphic to $\mathbb{Z} \times \mathbb{Z}/n \times \mathbb{Z}/2$. Additionally, though such dendrite groups will not have subgroups isomorphic to Γ, the dendrites will have infinite trees that suggest a subgroup isomorphic to $\mathbb{Z}/n * \mathbb{Z}/2$.

When m is at least three, however, we do not know enough to make any solid conjectures, and we will leave that problem open.

Bibliography

[1] James Belk and Bradley Forrest, *A Thompson Group for the Basilica*, Preprint (2010).

[2] Robert L. Devaney, *The Complex Dynamics of Quadratic Polynomials*, Proceedings of Symposia in Applied Mathematics (1984).

[3] Richard J. Thompson and Ralph McKenzie, *An Elementary Construction of Unsolvable Word Problems in Group Theory*, Studies in Logic and the Foundations of Mathematics (1973).

[4] J. W. Cannon, W. J. Floyd, and W. R. Parry, *Introductory Notes on Richard Thompson's Groups*, L'Enseignement Mathématique (1996).

[5] Victor Guba and Mark Sapir, *Diagram Groups*, Memoirs of the American Mathematical Society (1996).

[6] S. Morosawa, Y. Nishimura, M. Taniguchi, and T. Ueda, *Holomorphic Dynamics*, Cambridge University Press, Cambridge, UK, 2000.

[7] John Milnor, *Dynamics in One Complex Variable*, Princeton University Press, Princeton, NJ, 2006.

[8] Robert C. Gunning, *Lectures on Modular Forms*, Princeton University Press, Princeton, NJ, 1962.